



**Report of
the ASGASEX '94 workshop**

October 3-5, 1994

KNMI, De Bilt

the Netherlands

ed. by W.A. Oost

Technical report; TR-174

De Bilt, 1995

Postbus 201
3730 AE De Bilt
Wilhelminalaan 10
Telefoon 030-206 911 *
Telefax 030-210 407 **

(na 10-10-'95

* tel. +31(0)30-22 06 911
** fax +31(0)30-22 10 407)

UDC: (063)

551.46.062

551.526.63

551.506.24

ISBN: 90-369-2076-0

ISSN: 0169-1708

© KNMI, De Bilt. Niets uit deze uitgave mag worden verveelvoudigd en/of openbaar gemaakt worden door middel van druk, fotocopie, microfilm, of op welke wijze dan ook, zonder voorafgaande schriftelijke toestemming van het KNMI.

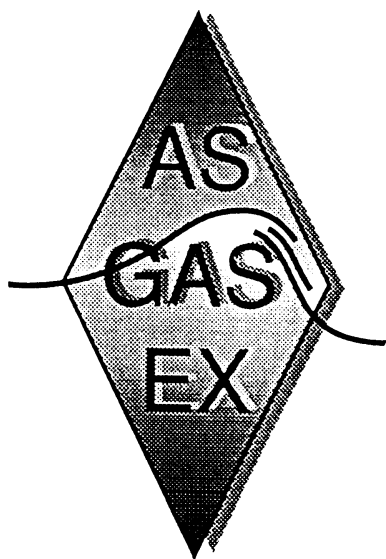
REPORT OF THE ASGASEX '94 WORKSHOP

October 3-5, 1994

KNMI

de Bilt

the Netherlands



CONTENTS	page
1. Introduction	1
2. Course of the workshop	2
3. ASGAMAGE	2
3.1 Instruments	2
3.2 Experimental schedule	3
4. Publications ASGASEX'93	6
5. Presentations	8
<i>Bob Anderson and Stu Smith (BIO):</i> A system for logging and processing air-sea interaction data	9
<i>Wim Kohsiek (KNMI):</i> Measurement and analysis of CO ₂ eddy fluxes with the KNMI sensor system.	11
<i>Gerard Kunz (TNO-FEL), Gerrit de Leeuw, Søren Larsen and Finn Hansen:</i> Eddy correlation fluxes of momentum, heat, water vapor and CO ₂ during ASGASEX.	12
<i>Stu Smith and Bob Anderson (BIO):</i> BIO Analysis of CO ₂ and H ₂ O flux in ASGASEX '93.	17
<i>Hein de Wilde (NIOZ):</i> N ₂ O and CH ₄ measurements during ASGASEX	22
<i>Dorothee Bakker, Hein de Baar and Bram Majoor (NIOZ):</i> CO ₂ air-sea exchange from air-sea concentration differences in the Dutch coastal zone.	28
<i>Gerrit de Leeuw (TNO-FEL) and Leo H. Cohen:</i> Size distribution of bubbles and aerosols	32
<i>David Woolf (SUDO):</i> Bubbles and vertical transport below the sea surface.	38
<i>Wiebe Oost (KNMI):</i> Trying to make it make sense.	42
<i>David Woolf (SUDO):</i> Investigating transport processes through the marine microlayer by passive thermal and radiometric methods.	48
<i>Phil Nightingale and Rob Upstill-Goddard (UEA/Newcastle):</i> Measurements of air-sea gas exchange using the dual tracer technique.	52
Annex 1 (Workshop agenda)	57
Annex 2 (Institute acronyms and participants)	60

**REPORT OF THE
ASGASEX/ASGAMAGE WORKSHOP
KNMI, DE BILT, THE NETHERLANDS
OCTOBER 3-5, 1994**

1. Introduction

The ASGASEX (for Air Sea GAS EXchange) experiment was held in September '93 on Meetpost Noordwijk (MPN), a research platform 9 km. (5 seamiles) off the Dutch coast, near the coastal resort of Noordwijk. The experiment was intended to identify and quantify factors affecting the air-sea exchange of atmospheric trace gases, in particular carbondioxide.

A central issue of the experiment was to measure fluxes of carbondioxide between sea and air using the so-called eddy correlation method. With this method it is possible, within certain restrictions, to measure directly the carbondioxide transport. The fluxes measured in this way were then to be related to a great number of other environmental parameters (Table 1) that were expected to be relevant to gas exchange at the sea surface.

Table 1. Measurements made at MPN during ASGASEX. Institute acronyms are explained in Annex 2

aerosol	TNO-FEL
air temperature	KNMI, BIO, TNO-FEL, RWS
alkalinity	NIOZ
bubbles	SUDO/UCG/IOSDL, TNO-FEL
CO ₂ flux	
eddy correlation technique	BIO, KNMI, TNO-FEL
gradient method	NIOZ
current, strength and direction	RWS
humidity	KNMI, BIO, TNO-FEL, RWS
humidity flux	KNMI, BIO, TNO-FEL
incoming short wave radiation	TNO-FEL
Langmuir circulations	SUDO/UCG/IOSDL
momentum flux	KNMI, BIO, TNO-FEL
N ₂ O, CH ₄ in air and water	NIOZ
pCO ₂ in air and water	NIOZ, BIO/DAL
rain	KNMI, TNO-FEL
sea water temperature	KNMI, RWS, NIOZ
sensible heat flux	KNMI, BIO, TNO-FEL
total CO ₂ in water	NIOZ
wave height	KNMI, RWS
whitecaps	KNMI
wind speed	KNMI, BIO, TNO-FEL, RWS

The objective of the present workshop was twofold: to discuss and compare the data from the '93 experiment and arrange for common publications as well as to prepare plans for a follow-up experiment, ASGAMAGE, the ASGASEX MAGE experiment. MAGE (Marine Aerosol and Gas Exchange) is a subgroup of IGAC, the International Global Atmospheric Chemistry programme, a subprogramme of IGBP, the International Geosphere-Biosphere Program of the United Nations.

ASGAMAGE is based on several motives. First, ASGASEX has only been a partial success, due to problems with the carbon dioxide fluctuation sensors, essential for the project, and to adverse weather conditions that limited both the amount and the quality of the CO₂ flux data. The ASGASEX data furthermore show some unexpected effects and trends that require more and more extensive data (and more study) for their analysis, which are discussed in what follows in the papers by Bakker (NIOZ) and by Oost (KNMI). A final reason to perform ASGAMAGE is the desire of several research groups to test their eddy correlation/accumulation instrumentation for flux measurements on various gases on a stable platform at sea, for which MPN provides a unique facility.

2. Course of the workshop

The workshop was attended by 18 people (see List of Participants). The programme of the workshop has been added as Annex 1. The first day and a small part of the second one were used for a presentation and discussion of the ASGASEX results. The presentations are summarized in section 5 of this report. The second day was mainly used to present and discuss an outline of the items to be addressed in ASGAMAGE within the (im)possibilities of the MPN platform and a dedicated ship operating in the neighbourhood. Planning and recommendations for ASGAMAGE are given in section 3. A short session on the third day sufficed to make the planning of ASGAMAGE as final as necessary and possible at this stage. The rather speedy progress was possible because of a large unanimity between the participants about the optimal programme within the constraints of the situation.

3. ASGAMAGE.

3.1. Instruments

All ASGASEX'93 participants (KNMI, BIO, TNO-FEL, NIOZ, UCG and SUDO) expressed their intention to participate again in ASGAMAGE with instruments comparable to or an extension of those used (in one or two cases: that were intended to be used) in the '93 experiment. NIOZ will furthermore apply for the ship "Pelagia" to be active during ASGAMAGE. An additional contribution of TNO-FEL could be a lidar to provide information about the atmospheric boundary layer. TNO-FEL will also operate instruments from Risø, as in ASGASEX; Risø will also make a contribution to ASGAMAGE in cooperation with MPIC.

New contributions may be expected from MPIC (Dr.S.Rapsomanikis), from UEA (Dr.P.Nightingale) and some related UK institutes and from one or more US institutes (represented by Dr.C.Fairall of NOAA, Boulder). The MPIC contribution is included in Table 2. The new UK contribution is a dual tracer experiment (see the lecture of Dr.Nightingale) on board a ship to the north of MPN. A preliminary US contribution is defined in Table 2; the flux measurements are for the time being intended to be made from MPN. The system to be used to that end, however, is being developed for use on a ship, so mounting it on the UK ship is not excluded. The wind profiler is to be mounted

aboard the UK ship anyhow.

Dr.D.M.Farmer of the Canadian Institute of Ocean Sciences has also indicated his interest in participation in ASGAMAGE. He was not present or represented at the meeting and will react later on the present planning. An indication for a possible contribution from IOS Canada is given in Table 2 with a question mark.

An intriguing result of ASGASEX was that a sizable fraction of pCO₂ results could be interpreted as indicating a vertical pCO₂ gradient in the upper meters of the water column (see the presentation by Oost). To confirm or refute this hypothesis two underwater pumps (instead of one as in ASGASEX) will be mounted during ASGAMAGE, at least one of which will be mounted in a way that allows easy variation of its vertical position. Another attempt to pin down what is going on in this respect is more attention to any biological processes affecting the CO₂ concentration.

In accordance with the ASGASEX philosophy several sets of CO₂ flux measurement systems (eddy correlation and/or eddy accumulation technique) will be operated simultaneously to be able to compare the results of these measurements, which are still at the very limit of what's technically possible. TNO-FEL and Risø will furthermore apply the inertial dissipation method.

3.2. Experimental schedule.

For several reasons the decision was taken to have two measurement periods, one in May, the other in October.

The May period (period 1) is important because of the maximum in the DMS production at that time and also gives information about other fluxes and gradients in the spring. It has the disadvantage of a - climatologically - low percentage of westerly (= onshore) winds. In the ASGASEX configuration this would also have meant very few direct flux measurements (with the eddy correlation or eddy assimilation technique), because the main instrument boom is mounted at the West side of the platform, which excludes flux measurements in winds with an easterly component, because of flow distortion. KNMI expects, however, to have an additional instrument arm operational on the North-West side of the platform during both ASGAMAGE periods, which will allow eddy correlation measurements in all winds with a northerly component.

The October period (period 2) is mainly a repetition and extension of ASGASEX, with pCO₂ measurements now being made at two levels in the watercolumn as indicated above. We expect the CO₂ flux sensors to perform better than during the former experiment when the two most sensitive systems were not ready in time, respectively suffering from technical problems. A valuable addition is the NOAA eddy accumulation system that in principle allows measuring fluxes of any non-reactive trace gas.

Splitting ASGAMAGE into two periods has the additional advantage that the berthing capacity of MPN (16 visitors) is not exceeded.

In connection with the suspicion of vertical CO₂ gradients KNMI will try to organize pCO₂/TCO₂ measurements at several levels in the watercolumn with a frequency of once every few weeks in the period before ASGAMAGE, starting as soon as possible. Whether this can be realized will depend on the cooperation of both RWS, which has to provide the facility to take the samples, and NIOZ or any other institute capable of doing the analysis.

Tables 3 and 4 summarize the platform visitors and their activities for both periods.

TABLE 2. INSTRUMENTS TO BE USED DURING ASGAMAGE.

INSTITUTE	INSTRUMENTATION
BIO	CO ₂ fluctuation sensor
BIO	Fast and slow temperature and humidity sensors
BIO	Sonic anemometer (Kaijo Denki)
IOS-Can.	Acoustics (bubbles), small buoys (?)
KNMI	Wave wire, breaking wave detection (video (2x), acoustic)
KNMI	CO ₂ fluctuation sensor, Fast and slow temperature and humidity sensors
KNMI	Rain detector
KNMI	Sonic anemometer (Kaijo Denki or Solent), Pressure anemometer
KNMI	1 underwater pump
KNMI/MPIC	2nd underwater pump
KNMI/NIOZ	3 air inlets for CO ₂ profile measurements
MPIC	Eddy correlation/accumulation system with GC for DMS, CH ₄ , N ₂ O (wind sensor optional)
MPIC	Li-Cor for pCO ₂ (equilibrator) and CO ₂ a, therosalinograph, fluorometer
NIOZ	2 equilibrators with GC's for CO ₂ , CH ₄ , N ₂ O
NIOZ	Coulometer, equipment for TCO ₂
NOAA	Eddy accumulation/correlation system
NOAA	Wind profiler (on ship)
RWS	Current meter, mooring and thermochain
RWS	WAVEC directional wave buoy
SUDO	2 radiometers
SUDO	O ₂ , C, T (near the pump inlet)
TNO/Risø	2 CO ₂ fluctuation sensors (Advantek)
TNO/Risø	Sonic anemometer (Solent)
TNO/Risø	BMS, Optical Particle Counter, Rotorods, Lidar, Raindetector, Pyranometer, Rotronic (on boom)
UCG/IOS-UK	Acoustics (bubbles), side scan (void fraction)

TABLE 3. PARTITION OF BERTHS AT MPN AMONG THE INSTITUTES.
(max. capacity 16)

Institute	Persons	Period	Persons Period 1	Persons Period 2
NIOZ	4	2		4
BIO(+DAL?)	3	2		3
MPIC/Risø	4	1	4	
SUDO	2	1	2	
UCG	1	1	1	
TNO/Risø	3	1,2	3	2
NOAA	2	2?		2
NCAR	1	1	1	
KNMI	4	1,2	4	4
Total			15	15

TABLE 4. PARAMETERS TO BE MEASURED DURING ASGAMAGE.

MPN:

Period 1:

<i>Institute(s)</i>	<i>Parameters</i>
MPIC/Risø	Fluxes of DMS, possibly CH ₄ , N ₂ O (eddy correlation/accumulation), pCO ₂ , CO _{2a}
MPIC/Risø	Salinity, water temperature, fluorescence
SUDO	Bubbles (acoustic), O ₂ , C, T, surface physics
UCG	Void fraction, breaking waves
TNO/Risø	4 fluxes, bubbles (optical), aerosol, lidar
KNMI	4 fluxes, waves, whitecaps, currents(RWS)

Period 2:

<i>Institute(s)</i>	<i>Parameters</i>
NIOZ	pCO ₂ (2×!), CO _{2a} , CH ₄ , N ₂ O, TCO ₂ , alkalinity, salinity, fluorescence, O ₂ , Ts
BIO/DAL	4 fluxes, pCO ₂ , CO _{2a}
TNO/Risø	4 fluxes, bubbles (optical), aerosol, lidar
NOAA	4 fluxes (eddy correlation/accumulation), wind profiler
KNMI	4 fluxes, waves, whitecaps, currents(RWS)

Ships: (1st and/or 2nd period)

UEA	Dual tracer experiment (<i>HMRS</i>)
NIOZ	Biological activity (" <i>Pelagia</i> ")

4 fluxes = fluxes of momentum, sensible heat, latent heat and CO₂

4. Publications ASGASEX '93

The meeting agreed on a policy with respect to the availability of ASGASEX data to third parties in the following way:

Until July 1996 ASGASEX data will only be made available to organizations or persons outside the ASGASEX programme after they have been published in the open literature.

The meeting furthermore agreed on a tentative publication scheme for the results of ASGASEX'93 as given in the following table. Publications will receive an ASGASEX serial number in order of receipt at KNMI of a copy of the first draft of the manuscript to be submitted to a journal. KNMI will handle the administration of these numbers.

Title/Subject:	Variability of dissolved oxygen in Dutch coastal waters
Author(s):	David Woolf, Duncan Purdie
1st draft ready:	End of '94
Journal:	Marine Chemistry
Title/Subject:	CH ₄ and N ₂ O in Dutch coastal waters: the influence of river input and air/sea gas exchange
Author(s):	Hein de Wilde, Wim Helder
1st draft ready:	End of '94
Journal:	Marine Chemistry
Title/Subject:	CO ₂ in Dutch coastal waters: hydrography and air/sea gas exchange
Author(s):	Dorothee Bakker, Bram Majoor, Hein de Baar
1st draft ready:	End of '94
Journal:	Marine Chemistry
Title/Subject:	Langmuir cells
Author(s):	Marcel Cure
1st draft ready:	1 July '95
Journal:	?
Title/Subject:	Vertical mixing
Author(s):	David Woolf, Marcel Cure
1st draft ready:	Summer '95
Journal:	Journal of Physical Oceanography
Title/Subject:	Bubble clouds and wave breaking
Author(s):	David Woolf, Marcel Cure, Gerrit de Leeuw
1st draft ready:	End of '95
Journal:	?
Title/Subject:	Moisture and other fluxes (no CO ₂)
Author(s):	Stu Smith, Bob Anderson, Wiebe Oost, Cor van Oort, Gerrit de Leeuw, Gerard Kunz
1st draft ready:	March '95
Journal:	Boundary Layer Meteorology

Title/Subject: Whitecaps, optical detection and modelling
Author(s): Rob Kraan, Wiebe Oost and Peter Janssen
1st draft ready: December '94
Journal: Journal of Atmospheric and Oceanic Technology

Title/Subject: Whitecaps and aerosol
Author(s): Gerrit de Leeuw, ?
1st draft ready: Summer '95
Journal: Journal of Geophysical Research

Title/Subject: Whitecap frequency and intermittency
Author(s): Marcel Cure, Rob Kraan (or Wiebe Oost)
1st draft ready: March '95
Journal: Journal of Geophysical Research

Title/Subject: Steady state and homogeneity requirements for CO₂ fluxes
Author(s): Chris Fairall, Stu Smith
1st draft ready: June '95
Journal: Boundary Layer Meteorology

Title/Subject: Synthesis paper for ASGASEX
Author(s): Wiebe Oost et (many) al
1st draft ready: March '96
Journal: ?

5. Presentations

(Institute acronyms can be found in Annex 2)

Bob Anderson and Stu Smith (BIO):

A system for logging and processing air-sea interaction data

Wim Kohsiek (KNMI):

Measurement and analysis of CO₂ eddy fluxes with the KNMI sensor system.

Gerard Kunz (TNO-FEL), Gerrit de Leeuw, Søren Larsen and Finn Hansen:
Eddy correlation fluxes of momentum, heat, water vapor and CO₂ during ASGASEX.

Stu Smith and Bob Anderson (BIO):

BIO Analysis of CO₂ and H₂O flux in ASGASEX '93.

Hein de Wilde (NIOZ):

N₂O and CH₄ measurements during ASGASEX

Dorothee Bakker, Hein de Baar and Bram Majoor (NIOZ):

CO₂ air-sea exchange from air-sea concentration differences in the Dutch coastal zone.

Gerrit de Leeuw (TNO-FEL) and Leo H. Cohen:

Size distribution of bubbles and aerosols

Marcel Cure (UCG) and Peter Bowyer:

Sonar study of surface turbulence (not available)

David Woolf (SUDO):

Bubbles and vertical transport below the sea surface.

Wiebe Oost (KNMI):

Trying to make it make sense.

David Woolf (SUDO):

Investigating transport processes through the marine microlayer by passive thermal and radiometric methods.

Phil Nightingale and Rob Upstill-Goddard (UEA/Newcastle):

Measurements of air-sea gas exchange using the dual tracer technique.

R.J.Anderson and S.D.Smith (BIO):
A system for logging and processing air-sea interaction data

The ASGASEX 93 Experiment was the first in which we used a new software system in Turbo Pascal for logging and processing time series data for eddy and dissipation fluxes. This system produces spectral and flux analyses a few minutes after completion of a data run. A wide range of data processing options is controlled by a "configuration file", and data runs can be quickly and easily reprocessed with different options by modifying this file.

The hardware for this system consists of a 486 personal computer with two 12-bit Keithley-Metrabyte DAS-8-PGA boards to accept up to 16 analog input channels.

Instrumentation deployed on the MPN boom during ASGASEX consisted of a Kaijo Denki sonic anemometer-thermometer, micro-thermistors, and a Lyman alpha hygrometer. A new IR CO₂/H₂O sensor developed by M. Moschos for Agriculture Canada was unfortunately not ready in time for the experiment. Signals from two other IR CO₂/H₂O sensors (Risø's Advanet operated by TNO, and KNMI's IFM) were recorded, and also the KNMI aspirated Lyman alpha hygrometer and sonic anemometer. In addition to the usual tilt corrections to the wind data, time shifts have been applied to adjust for along-wind sensor separation and for time delays of certain sensors, resulting for example in sonic W signals that remain coherent and in-phase at frequencies up to 3 Hz (Fig. 1). These can be used interchangeably in eddy flux calculation, in spite of their 2 m separation at opposite prongs of the boom. Calibrations have been matched using the lower-frequency part of the spectra. No corrections for flow distortion by MPN nor for local flow distortion have been applied to the results shown.

Although water vapour signals from the different IR and Lyman alpha hygrometers were highly coherent and gave good agreement, the coherence of the two IR CO₂ signals was low (e.g. Fig. 2), showing that except at the lowest frequencies (0.007-0.05 Hz) the signals did not represent the same fluctuations. It is possible to obtain a good eddy flux from a noisy signal as long as the noise is not correlated with the vertical wind, but we will see later that the KNMI CO₂ flux was systematically more positive, typically by the order of 0.1 mg/ms.

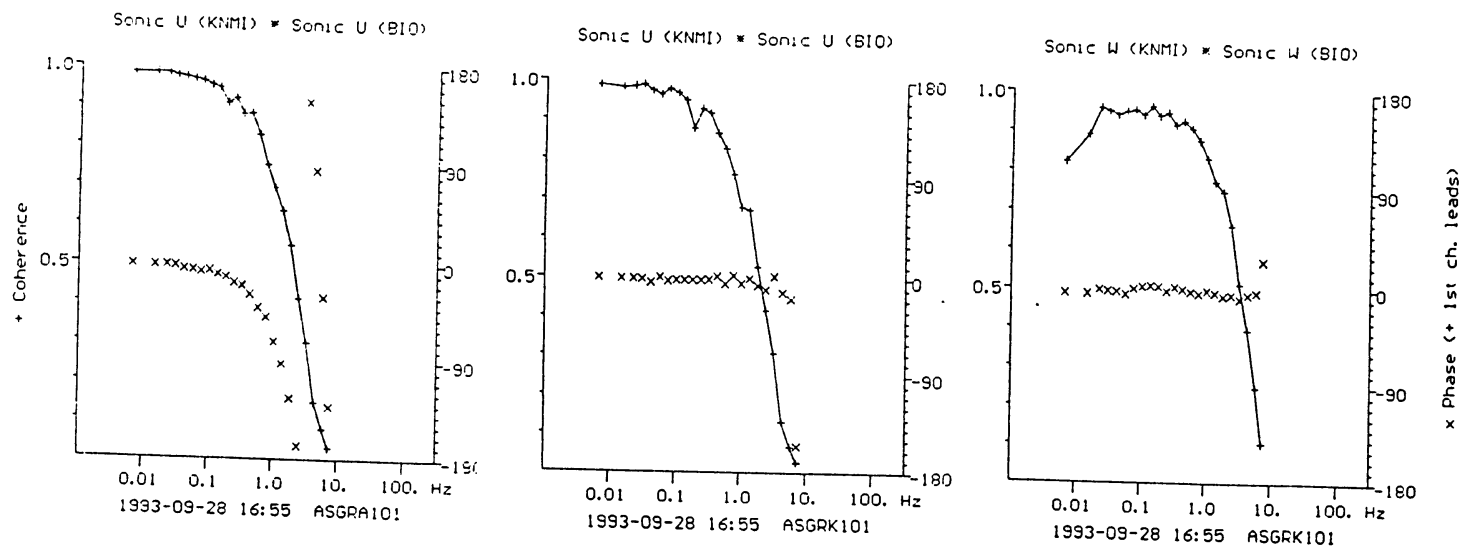


Fig. 1. Coherence and phase of sonic anemometers at 2 m separation: (a) U before, (b) U after time lag, and (c) W after time lag correction, for BIO run 101 starting at 1655 GMT 28/09/93.

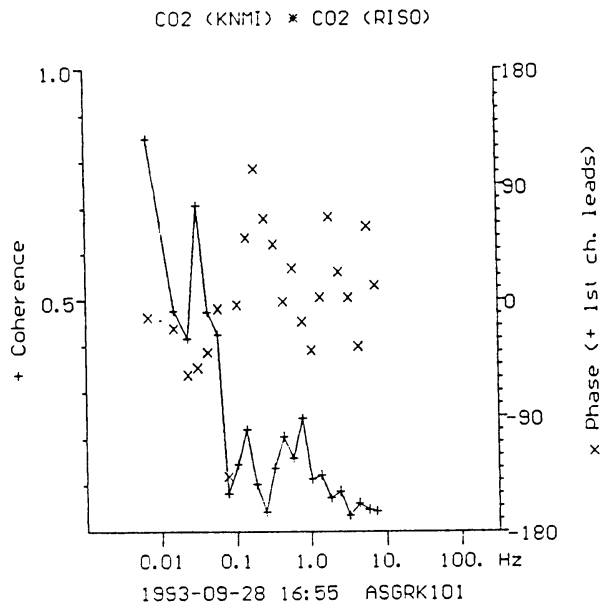


Fig. 2. Coherence and phase of IR CO₂ from KNMI IFM and TNO-Risø Advanet.

Wim Kohsiek (KNMI):

Measurement and analysis of CO₂ eddy fluxes with the KNMI sensor system.

Factors affecting the accuracy of the eddy correlation CO₂ measurements were discussed, in particular:

- instrument exposure
- calibration
- cross-talk from H₂O
- the Webb correction
- the effect of impurities (droplets, salt) on optics.

The exposure correction was shortly dealt with. Reference was made to publications by Oost. Corrections for the flow distortion by the boom head were made with a model treating the obstacles as ellipsoids, whereas the distortion offered by the platform had been investigated earlier in the course of the HEXOS program by means of wind tunnel studies.

The infrared sensor (IFM) was laboratory calibrated by putting the sensing head in a chamber. The air inside the chamber was varied in CO₂ concentration and in H₂O concentration. Care was taken that the calibration cycles were performed as rapidly as possible to avoid effects from sensor drift. The overall accuracy of the calibration, including curve-fitting, was estimated at 5% for both CO₂ and H₂O.

Cross talk from water vapor was investigated by splitting a stream of gas (N₂ with a known content of CO₂) into two parts, and leading each leg to a water saturator. The temperature difference between the saturators was 7 °C. The IFM was quickly switched from one air stream to the other. Within the accuracy of the experiment no cross talk could be detected. If cross-talk is present, it should be less than 0.0002 g/cm³ CO₂ per g/m³ H₂O.

For the majority of the runs the Webb correction was considerable and of the same magnitude as the uncorrected fluxes. Heat flux and water vapor flux were about equally important in this correction. As these fluxes were always directed away from the sea surface, the correction is positive. Most raw CO₂ fluxes were negative, after correction, however, they were generally positive.

When it was raining, the apparent CO₂ fluctuations were large and very strongly correlated with H₂O fluctuations. It was argued that droplets or water films on the optics may occasion extra absorption in the CO₂ infrared channels, and lead to a false signal. This point was illustrated by time recordings of CO₂ and H₂O, with and without rain, and the power spectra for these runs.

It was noted that the IFM spectra exhibit electromechanic noise at about 2Hz. The cospectra for vertical wind speed and CO₂ suggest that little covariance is contributed by frequencies above 0.1Hz.

The overall conclusion was that, considering the sources of errors mentioned above, the observed CO₂ fluxes of 0 to 0.1 mg/m²s² were above the noise level.

Eddy correlation fluxes of momentum, heat, water vapor and CO₂ during ASGASEX

G.J. Kunz, G. de Leeuw
TNO Physics and Electronics Laboratory
2597 AK The Hague, The Netherlands

S.E. Larsen, F.Aa. Hansen
RISØ National Laboratory
Department of Meteorology and Wind Energy
Roskilde, DK-4000, Denmark

1. INTRODUCTION

During ASGASEX, TNO-FEL operated a micrometeorological flux package consisting of an ultrasonic anemometer (Solent) and two open path infrared H₂O and CO₂ concentration fluctuation meters (Advanet, E009A). The instruments were mounted upside down on the South side of the prong at the end of the 21 m boom, with their sampling volumes 67 cm (Sonic) and 25 cm (Advanet) below the boom; horizontal separation between the two gas sensors 20 cm and distance to the anemometer 25 cm. The ultrasonic anemometer was tested in a wind tunnel [Kunz, 1994]. During the experiment, the CO₂ channels of the gas sensors were calibrated on a regular base using N₂ and two factory-calibrated gas mixtures with respectively 250 ppm and 450 ppm CO₂ (balance nitrogen). For water vapor, the factory calibration was used.

The data were sampled with a frequency of 20 Hz in blocks of 45 minutes duration and converted to physical parameters. The wind vector was transformed to a new orthonormal system with zero mean vertical wind and one streamwise wind component. One minute mean values and covariances of meteorological parameters and fluxes of momentum, sensible heat, latent heat and carbon dioxide were calculated. The results were compared with existing models, with results of other experiments and with results obtained by other groups participating in ASGASEX.

Altogether, 102 45-minute data blocks were recorded with the sonic from which 63 in combination with the Advanets. Thus far, no selection has been made for special conditions except for comparison with data from other participants. During BIO run numbers 55 and 56, the Solent did not operate properly.

Because TNO's Advanet did not operate properly, the proposed method to suppress incoherent noise by combining two gas sensors, could not be tested. Evidently, the results presented are therefore based on the Advanet owned by RISØ, Denmark.

2. RESULTS

2.1 Wind and momentum flux

The sonic data were corrected for tidal currents and transformed to U_{10N}, the wind speed at the standard altitude of 10 m in neutral conditions. The friction velocity u* was directly determined from the Sonic wind components. The neutral drag coefficient, $C_{DN} = u_*^2 / U_{10N}^2$, derived from these data is presented in Figure 1 and compared with the HEXOS data recorded at the same location [Smith *et al.*, 1992]. The discrepancy at wind speeds exceeding 10 m/s is not understood.

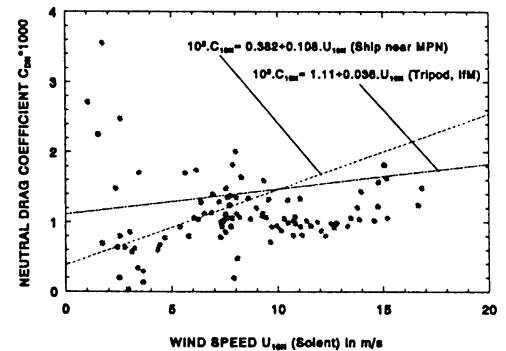


Figure 1. Neutral drag coefficients, C_{DN} , as a function of wind speed. HEXOS results have been indicated.

2.2 Temperature and sensible heat flux

Air temperatures were derived from the speeds of sound and corrected for humidity [e.g. Schotanus *et al.*, 1983]. Heat fluxes ($H = \rho C_p \langle w'T \rangle$) were derived by cross correlating time series of vertical wind speed and temperature, both provided by the sonic. The relation between the scaling temperature, ($T_* = H/u_*$), and the air-sea temperature difference is presented in Figure 2 and compared with a relation presented by Davidson, 1978. Figure 3 shows the relation between the kinematic heat

the line in this figure represents the Dalton number, the bulk transfer coefficient for moisture.

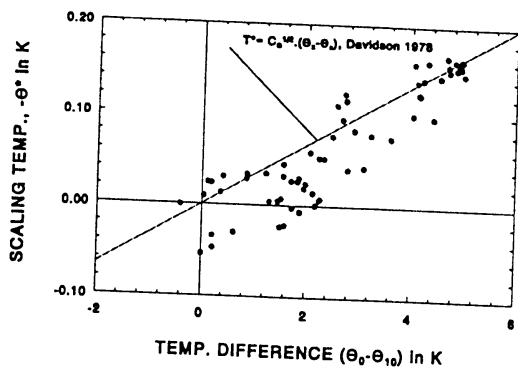


Figure 2. Scaling temperature, T^* , versus the air-sea temperature difference.

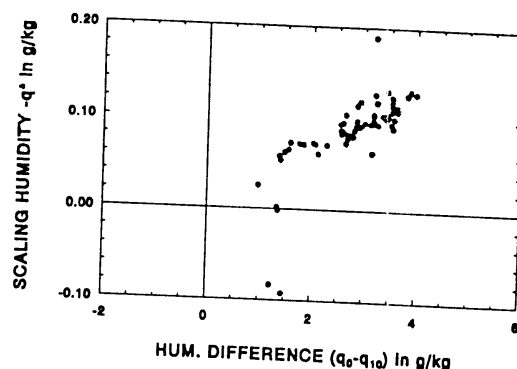


Figure 4. Scaling humidity, q^* , derived from data provided by the Solent and the water vapor channel of the Advanet, as a function of the humidity gradient using the MPN data.

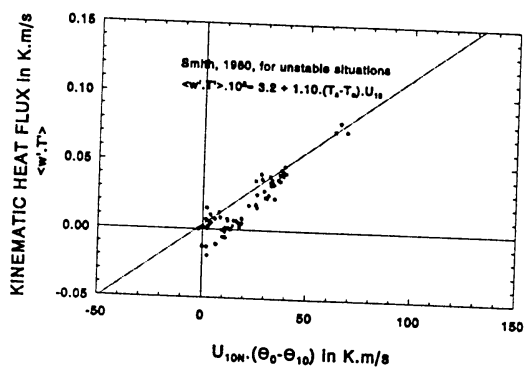


Figure 3. Kinematic heat flux versus the product of wind speed and air-sea temperature difference.

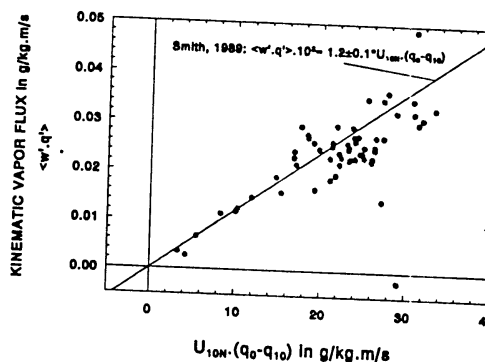


Figure 5. Kinematic water vapor flux, derived from data provided by the Solent and the water vapor channel of the Advanet, as a function of the product of wind speed and humidity difference between 0 and 10 m altitude.

flux, $\langle w'T^* \rangle$, and the product of wind speed and air-sea temperature difference. The slope of the line in this figure represents the Stanton number, the bulk transfer coefficient for heat.

2.3 Humidity and water vapor (latent heat) flux

Time series from the water vapor channel of the fast response IR gas sensor and from the vertical component of the sonic anemometer were cross correlated to determine water vapor fluxes, $E = \rho \langle w'q' \rangle$. Figure 4 shows a scatterplot of the scaling humidity ($q^* = E/u_*$) as a function of the humidity difference between 0 and 10 m altitude. The relative humidities were taken from the MPN data set. The relation between the kinematic water vapor flux, $\langle w'q' \rangle$, and the product of wind speed and humidity difference between 0 and 10 m altitude is shown in Figure 5. Also the results of Smith, 1989, are shown. The slope of

2.4 Carbon dioxide and carbon dioxide flux

Atmospheric background concentrations of CO₂ could be measured with the Advanet because the sensor was calibrated absolutely on a regular base. In Figure 6, these data have been compared with the gas-chromatograph data (NIOZ) which were converted to absolute atmospheric concentrations.

To understand the systematic differences between the two sensors, the two data sets were compared with different meteorological parameters. Some correlation was found with relative humidity and wind direction as shown in Figures 7 and 8. The dependence on relative humidity might indicate cross talk of water vapor into the carbon dioxide channel of the Advanet.

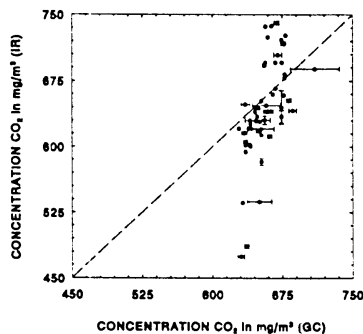


Figure 6. Comparison of the atmospheric background concentration CO₂, measured with the absolutely calibrated Advanet (RISO) and with the gas-chromatograph (NIOZ).

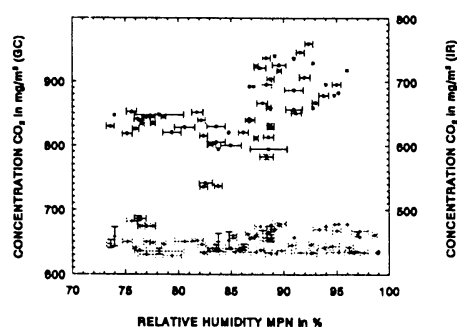


Figure 7. Atmospheric CO₂ background concentration measured with the Advanet (solid circles) and with the gas-chromatograph (plus signs) as a function of the relative humidity.

Figure 8 shows that the largest concentrations were measured during Southerly winds (Rotterdam industrial region, 'Westland' greenhouses and the densely populated areas) and lowest concentrations during Northerly winds (oceanic air mass). Combination of Figures 7 and 8 indicates that Southerly winds transported air masses with the highest relative humidities.

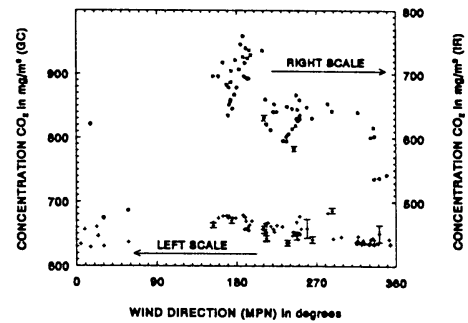


Figure 8. Atmospheric CO₂ background concentration measured with the Advanet (solid circles) and with the gas-chromatograph (plus signs) as a function of the wind direction.

Time series of the CO₂ gas and the vertical wind component of the Solent were cross correlated to determine the 'raw' vertical CO₂ fluxes, $F_r = \langle w \cdot c \rangle$. These fluxes were corrected for density variations due heat and water vapor, generally called 'Webb correction'. See Smith and Jones, 1979, and Webb, Pearman and Leuning, 1980. In Figure 9, the 'net' CO₂ fluxes are compared with the 'net' fluxes calculated by BIO using the same Advanet but a different sonic and two different analysis methods. Taking into account the turbulent behaviour of the signals and the complexity of the analysis, the agreement is excellent.

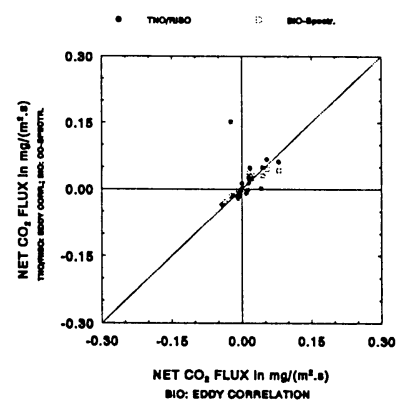


Figure 9. Corrected TNO/RISO CO₂ fluxes (Advanet/Solent) versus the BIO CO₂ fluxes (Advanet/Kayo Denki) (solid circles, eddy correlation fluxes; open squares, co-spectra results).

In analogy with fluxes of heat and water vapor, the CO_2 fluxes were compared with the air-water CO_2 concentration difference ($\Delta p\text{CO}_2$) and with the product of this difference and wind speed. Figure 10 shows the scaling CO_2 fluxes ($F_c^* = F_c/u^*$) as a function of $\Delta p\text{CO}_2$, which was independently measured by NIOZ. Figure 11 shows a scatter diagrams of the CO_2 fluxes as a function of the product of wind speed and $\Delta p\text{CO}_2$, NIOZ.

Figure 12 shows a relation between the CO_2 fluxes and the wind speed.

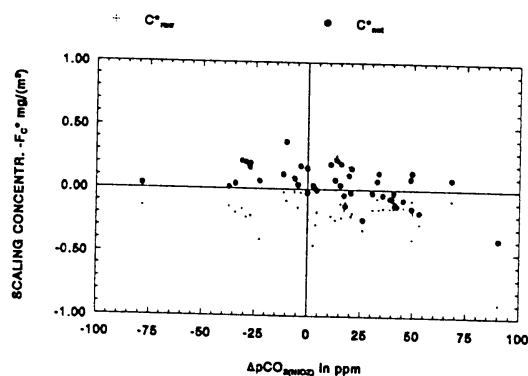


Figure 10. Corrected (solid circles) and uncorrected (small plus signs) TNO/RISO scaling CO_2 fluxes, F_c^* , versus $\Delta p\text{CO}_2$ (NIOZ).

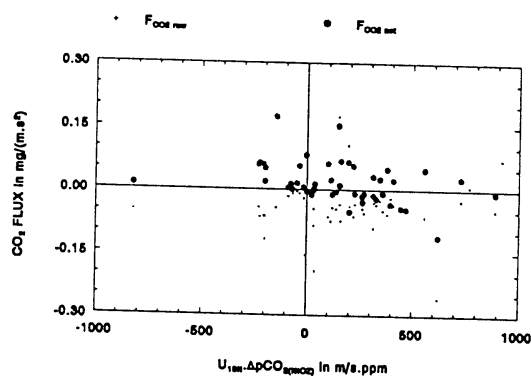


Figure 11. Corrected (solid circles) and uncorrected (small plus signs) TNO/RISO CO_2 fluxes versus product of wind speed and NIOZ sea-air CO_2 concentration difference.

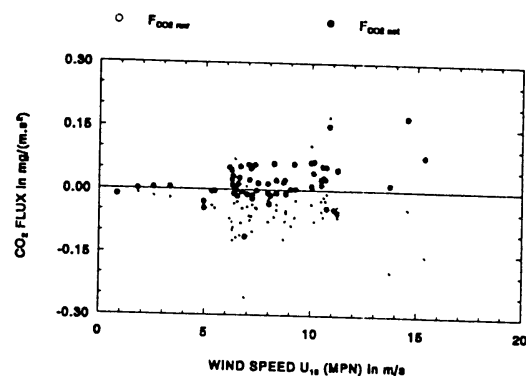


Figure 12. Corrected (solid circles) and uncorrected (small plus signs) TNO/RISO CO_2 fluxes as a function of wind speed.

3. CONCLUSIONS

During ASGASEX, excellent and valuable data were obtained for modelling fluxes of momentum, heat and water vapor. Values for C_D , C_H and C_E compare with those found in literature. Also the scaling temperature and humidity parameters were comparable with existing models. This gave us confidence in the data measured with our micrometeorological package.

Using a regularly calibrated fast response infrared gas sensor, the atmospheric background concentration of CO_2 was measured and compared with the results from a relatively slow responding gas-chromatograph. The results of both instruments have shown that the CO_2 concentration depends on the wind direction. Some cross talk due to water vapor cannot be excluded.

The measured net CO_2 flux values varied from -0.03 to +0.07 $\text{mg}/(\text{m}^2.\text{s})$, but were generally positive. CO_2 flux measurements over land in November 1993 at Cabauw, indicated that the flux that could be resolved with the sensor package was about 0.02 $\text{mg}/(\text{m}^2.\text{s})$ [Kunz, 1994]. We therefore conclude that the signal-to-noise ratios do not exceed a factor 3.5. Nevertheless, the net CO_2 fluxes calculated by TNO/RISO package compare reasonably well with the independently derived net fluxes from the BIO package.

The CO_2 fluxes could not be modelled in a similar way as the scalar fluxes of sensible heat and water vapor. It seems that there is only a slight dependence on wind speed over the range of wind speeds experienced during ASGASEX. This is in agreement with existing models.

ACKNOWLEDGEMENT

The authors realize that the success of ASGASEX and the quality of the final results depend heavily on contributions from many people. We first want to acknowledge the excellent support given the crew of MPN. We also thank Wiebe Oost and Rob Kraan of KNMI for the opportunity to participate in this experiment and for the logistic support to mount our micrometeorological instruments on the boom. We are very grateful to Stu Smith for his stimulating initiatives, pleasant discussions and willingness to exchange results during the whole data analysis period. In this context, we are also indebted to Ken Davidson on visit from the Naval Post Graduate School, Monterey, USA, during the summer of 1994. Main technical support was received from Leen Bruinsma, Leo Cohen and Marcel Moerman (TNO-FEL) and from Cor van Oort and Rob Cornet (KNMI). We also acknowledge Drs. W. Pelt of the Royal Dutch Navy for his efforts to support our contributions to ASGASEX. This work was done under the OMEX contract MAS2-CT93-0069 of the European Commission and contract A92KM767 of the Netherlands Ministry of Defence.

REFERENCES

- Davidson, K.L., T.M. Houlihan, C.W. Fairall and G.E. Schacher, 'Observation of temperature structure function parameter, C_T^{-2} , over the ocean' *Bound.-Layer Meteor.*, 15, 507-523, 1978.
- Kunz, G.J. 'Tests of a GILL ultrasonic anemometer (Solent) in a wind tunnel' TNO-Physics and Electronic Laboratory, FEL-94-A118, 1994.
- Kunz, G.J., 'TNO-FEL contributions to a pilot experiment for CO₂ flux measurement comparisons' TNO-Physics and Electronics Laboratory, FEL-94-163, 1994.
- Schotanus, P., F.T.M. Nieuwstadt and H.A.R. DeBruin, 'Temperature measurement with a sonic anemometer and its application to heat and moisture fluctuations' *Bound.-Layer Meteor.*, 26, 81-93, 1983.
- Smith, S.D. and E.P. Jones, 'Dry-air boundary conditions for correction of eddy flux measurements' *Bound.-Layer Meteor.*, 17, 375-379, 1979.
- Smith, S.D., 'Water vapor flux at the sea surface; Review paper' *Bound.-Layer Meteor.*, 47, 277-293, 1989.
- Smith, S.D., R.J. Anderson, W.A. Oost, C. Kraan, N. Maat, J. DeCosmo, K.B. Katsaros, K.L. Davidson, K. Bumke, L. Hasse and H.M. Chadwick, 'Sea surface wind stress and drag coefficients: the HEXOS results' *Bound.-Layer Meteor.*, 60, 109-142, 1992.

- Webb, E.K., G.I. Pearman and R. Leuning, 'Correction of flux measurements for density effects due to heat and water vapour transfer' *Q.J.R. Meteorol. Soc.*, 106, 85-100, 1980.

S.D. Smith and R.J. Anderson (BIO):
BIO Analysis of CO₂ and H₂O flux in ASGASEX '93.

Dalhousie DpCO₂ system.

In addition to the eddy flux system, Dalhousie University (Owen Hertzman, Manon Poliquin and Marie-Claude Bourque) deployed an equilibrator system for measuring DpCO₂. It was similar in concept to the NIOZ system except that a Li-Cor IR gas analyser was used instead of a gas chromatograph. (NIOZ now also uses a Li-Cor.) In spite of the similarity, the two systems gave very different values of DpCO₂ (Fig. 1). An intercomparison will be done at NIOZ later in 1994 to ensure that in the future experiments the two systems can be expected to give equivalent results within a few ppm.

Wind stress, heat flux and evaporation.

Wind stress and heat flux coefficients from ASGASEX (Figs. 2, 3, 4) replicate the HEXOS results. Deleting the cases with rain, the range of wind speeds is from about 4-13 m/s. Evaporation measured with the bare and aspirated Lyman alpha hygrometers, and with two IR sensors, agrees closely and the mean value of $C = 0.00123$ is 8% higher than the mean from HEXOS, well within the scatter.

CO₂ flux.

Cospectra of CO₂ and W (Fig. 5) illustrate the systematically higher flux derived from the IFM as compared to the Advanet sensor. Each point in the time series has adjustments for thermal and water vapour dilution equivalent to the well-known "Webb correction", so that the area between the cospectrum and the axis is an estimate of the CO₂ flux. Interchanging the anemometer signals (i.e. between opposite prongs) has relatively little effect since all signals have been adjusted for time delays due to downwind displacement. Problems with drift of the Advanet sensor were noted, so that the integral of the cospectrum (i.e. not including frequencies < 0.006 Hz) is considered to be a better estimate of the CO₂ flux than the total covariance. Time series of DpCO₂, DT, DQ, U and CO₂ flux on Sept. 21 and 28 were discussed.

A plot of Advanet CO₂ flux for all runs (excluding rain, which affects the optics of the open-path IR sensors), against the product ($U \times DCO_2$), suggests a line with positive slope which could be equated to an exchange coefficient (Fig. 6). The KNMI flux is higher, typically by about 0.1 mg/m²s. However, if the NIOZ values of DCO₂ (considered to be more reliable) are used instead (Fig. 7) the slope is reversed, and a negative slope would lead to the un-physical result of a negative exchange coefficient. At this stage the results do not yield a consistent value for an exchange coefficient in the conventional sense. On the other hand, they also show that with an order of magnitude improvement of the noise level of CO₂ sensors now nearing completion and with the rather high values of DpCO₂ often found at MPN, it will be possible to make reliable CO₂ eddy flux measurements.

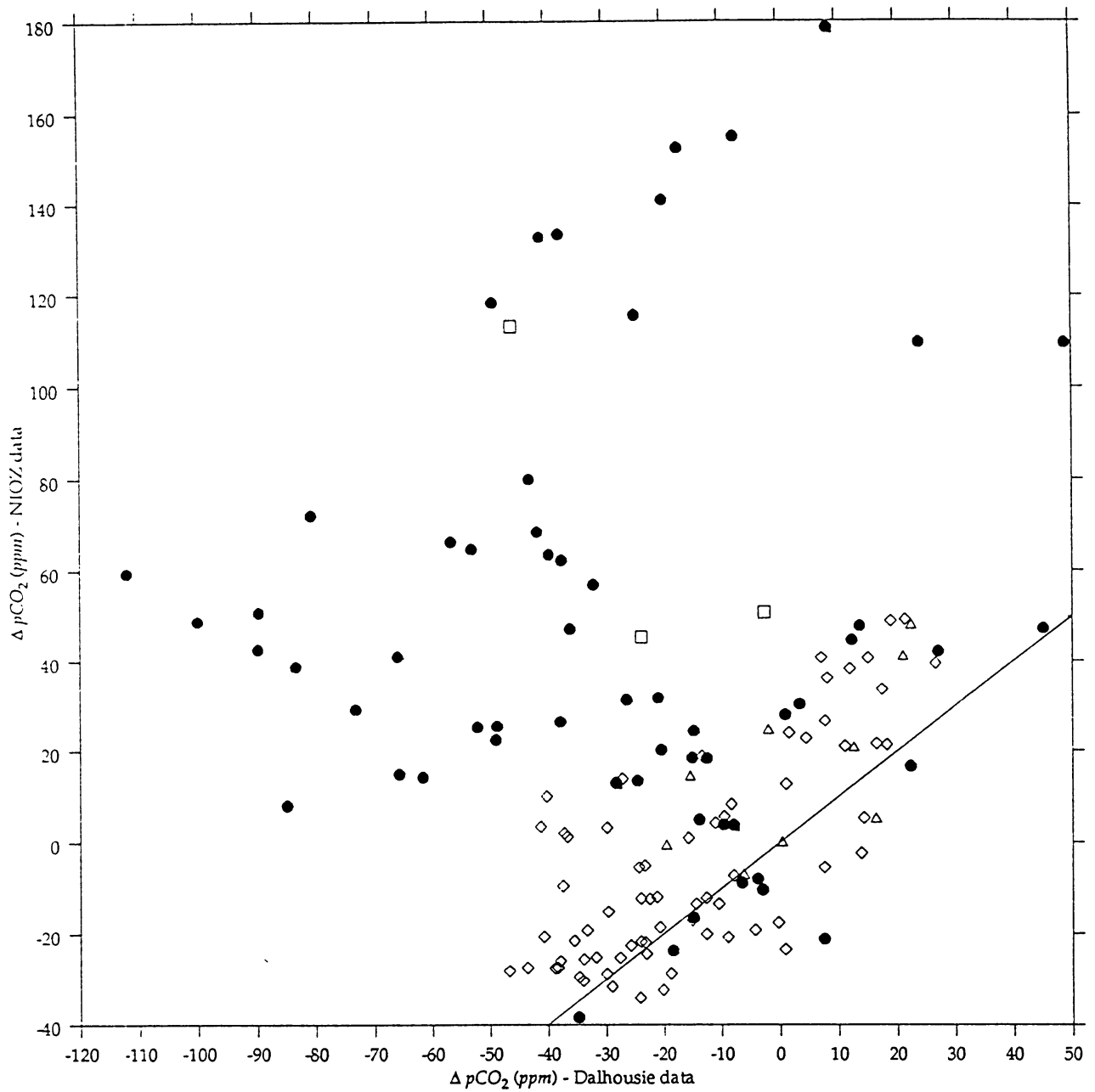


Fig. 1. $\Delta p\text{CO}_2$ from Dalhousie and NIOZ systems, during the first (Δ), second and third (Smith, \square ; Bourque \circ) and last week (Hertzman, \diamond). The largest differences were during the middle period, but consistent agreement within a few ppm was never achieved.

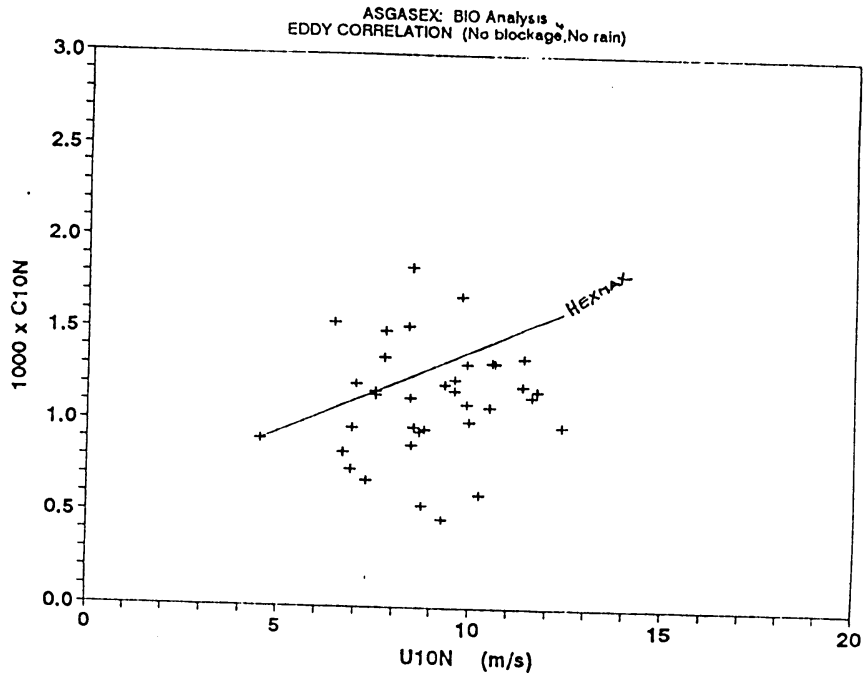


Fig. 2. Drag coefficients from the BIO sonic anemometer, adjusted to neutral stability and 10 m height. The line is a combination of results from KNMI PA, Kaijo sonic, and UW K-Gill anemometers in HEXMAX. Four low outliers represent north wind cases where the anemometer, on the south prong of the boom, was blocked by other sensors.

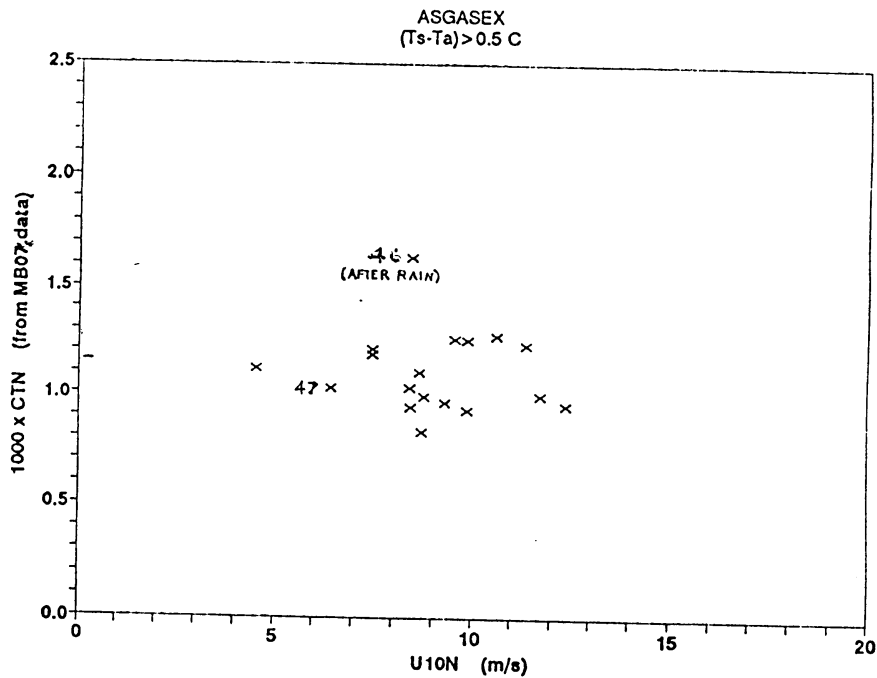


Fig. 3. Heat flux coefficients from BIO thermistor and sonic anemometer, adjusted to near-neutral stability and 10 m height. Cases with rain or severe flow blockage are deleted. One high outlier (BIO run 47) immediately followed a period of rain.

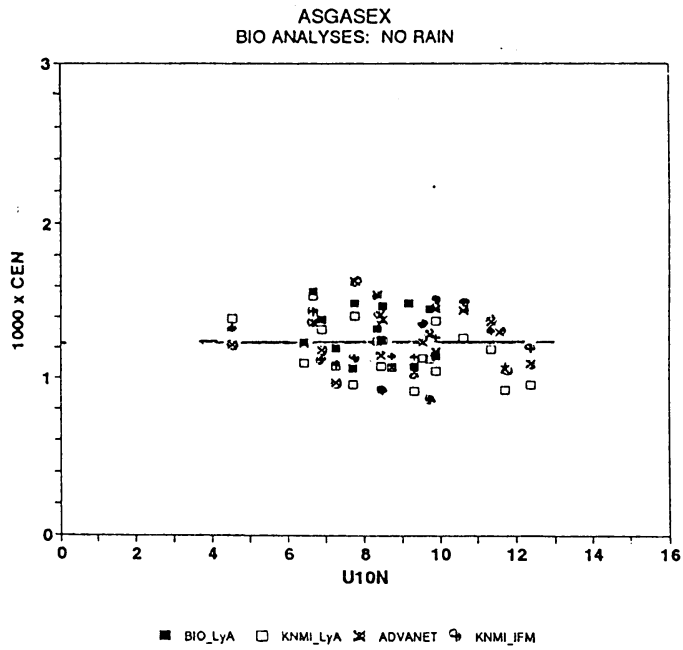


Fig. 4. Evaporation coefficients adjusted to neutral stability and 10 m height, from four hygrometers. Cases with rain or severe flow blockage are deleted. The mean value is $(1.23 \pm 0.18) \times 10^{-3}$.

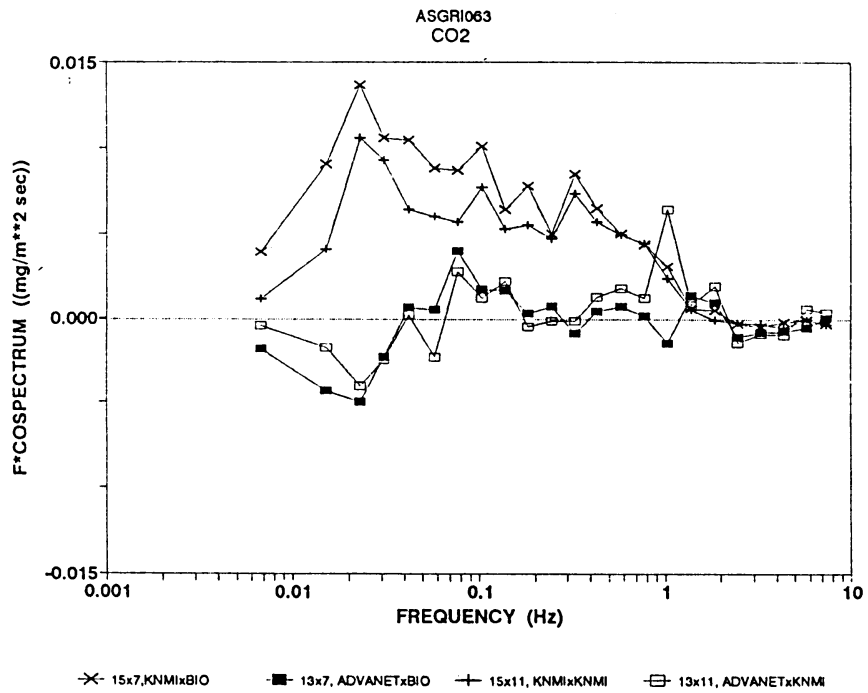


Fig. 5. Cospectra of CO₂ flux.

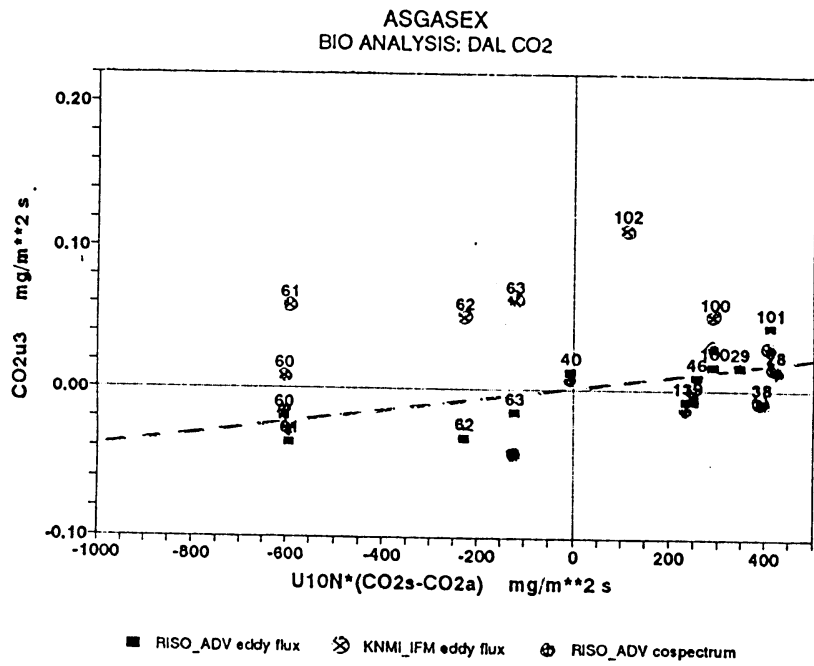


Fig. 6. CO₂ flux vs. (U × DCO₂), Dalhousie data. The slope of a line fitted to these points would suggest an exchange coefficient $C_{CO_2} \sim 0.04 \times 10^{-3}$.

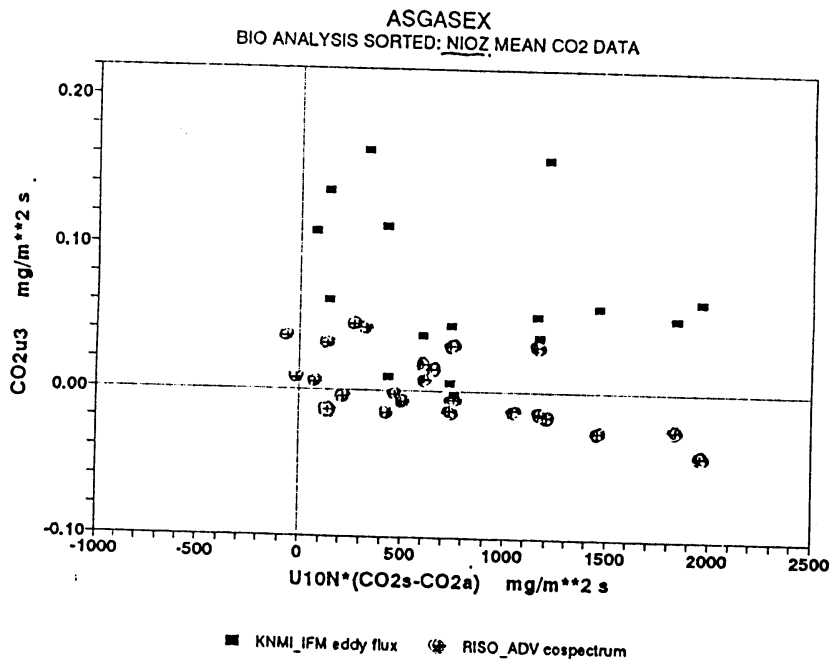


Fig. 7. CO₂ flux vs. (U × DCO₂), NIOZ data. The Advanet data would now indicate a negative exchange coefficient.

N₂O and CH₄ measurements during ASGASEX

H.P.J de Wilde

Netherlands Institute for Sea Research (NIOZ)

In co-operation with D.C.E Bakker and B. Majoor (NIOZ)

With support of the KNMI team

1 Introduction

Nitrous oxide (N₂O) and methane (CH₄) are important radiatively active trace gases. N₂O also contributes to ozone depletion and the formation of acid-rain (IPCC, 1992; Badr and Probert, 1993). The influence of the marine environment on the global budgets of both N₂O and CH₄ is presently poorly quantified, indicating the necessity of more marine studies.

Within the framework of the international Air Sea GAS EXchange experiment (ASGASEX; Oost 1994) N₂O and CH₄ concentrations in surface water and the atmosphere were monitored during September 1993 on a platform located 10 km off the Dutch coast (Meetpost Noordwijk). In contrast to shipboard measurements, the platform offered the unique possibility of monitoring *temporal* variations in the concentrations of dissolved and atmospheric trace gases as well as the resulting water-atmosphere exchange.

2 Methodology

Analytical system

Analyses were carried out on a gas chromatograph (Chrompack CP9000) which was modified for automated sample selection and for combined N₂O and CH₄ analysis in the same sample. Calibration was done by analysis of combined N₂O/CH₄ working standards (252/1400, 506/2800, and 1475/8400 $\mu\text{mol/mol}$ N₂O/CH₄ in synthetic air). Working standards were calibrated against gravimetrically prepared primary N₂O standards of 300 and 1198 ($\pm 1\%$) nmol/mol N₂O in synthetic air (Nederlands Meetinstituut, Delft) and CH₄ standards of 913 and 2280 nmol/mol in synthetic air (NIST, USA).

The precision of the various measurements, expressed as the relative standard deviation, is typically 0.6% (N₂O)/ 0.4 % (CH₄) for atmospheric samples and about 1.5% (N₂O)/ 1.0 % (CH₄) for equilibrator samples.

Sampling

Surface water concentrations were monitored with a continuous equilibration system comparable to a system described by Robertson et al. (1992). Sea water from 5 m depth was continuously pumped up and sprayed through a fixed volume of air, which was periodically analysed on the gas chromatograph.

This equilibrator-system was extensively tested and found to have a response time for CH₄ equilibration between 15 and 25 minutes, depending on the water throughput. The response times for gases with higher solubilities, such as N₂O and CH₄ is likely much smaller (order of minutes) as the solubility of N₂O is much higher than of CH₄. The water temperatures at the pump inlet and in the equilibrator were monitored to correct for slight solubility changes due to warming in the piping and pumping system.

Atmospheric concentrations were determined by sampling and analysing air that was pumped through gas-tight tubing (Decabon) from the end of 'the boom' and from additional inlets positioned at various levels above the water surface. Atmospheric samples were not dried. Instead, relative humidity and air temperature were used to calculate dry air mixing ratios of N₂O and CH₄ by correcting for water vapour pressure.

Calculations

Computations of the partial pressure differences of dissolved gases in surface water with respect to their atmospheric values (i.e. the driving potential for gas exchange), are based on calculated surface water solubilities according to the temperature-salinity-solubility relationships of Weiss and Price (1980) for N₂O, and Wiesenburg and Guinasso (1979) for CH₄. Water-atmosphere fluxes were computed by combining the measured air-sea partial pressure differences with common relationships between wind speed, temperature and gas transfer (Liss and Merlivat, 1986; Wanninkhof, 1992). Unfortunately the inevitable use of these parameterised gas transfer relationships introduces significant uncertainties in the estimated fluxes. Erickson, (1988) estimated that uncertainties in wind speed, water temperature, and calculations alone introduce an error of at least 50%.

Gradient technique

Additional CH₄/N₂O flux measurements were made with the aerodynamic gradient technique (in co-operation with J.H. Duyzer, TNO-

Environmental Sciences, Delft). Concomitantly with some of the KNMI runs, marine air from 3 levels above the water surface was sampled for 45 minutes in 60 l gas-tight bags. Multiple analysis ($n \approx 40-75$) of the sampled air was necessary as the required precision for this technique is high. Like the eddy correlation method, which was applied for CO₂ measurements, the gradient technique offers the advantage that it makes no use of a parameterised air-sea gas transfer velocity.

3 Preliminary Results

CH₄

The measured concentrations of dissolved CH₄ were remarkable high, causing surface water saturations of up to 30 times with respect to the atmosphere. The CH₄ saturation was found to be related to the tide, resulting in periodically fluctuating emissions (see figure). Tropospheric CH₄ concentrations were occasionally significantly elevated during conditions of easterly winds.

A preliminary evaluation of the flux measurements by the gradient technique indicated CH₄ fluxes between 2,5 and 10 $\mu\text{g}^{-2} \text{m}^{-2} \text{s}^{-1}$. This seems in reasonable agreement with the expected values based on the air-sea partial pressure differences. However, a direct comparison between the different methods for measuring air-sea gas exchange is significantly complicated by the large fetch area of the gradient measurements and the inhomogeneity of the water masses around the platform.

The very high CH₄ concentrations measured during ASGASEX initiated field work focused on a potential riverine origin of CH₄ in coastal waters. Closely after ASGASEX CH₄ measurements were made in the Scheldt river/estuary (in co-operation with J. Middelburg, Netherlands Institute of Ecology, Centre for Estuarine and Coastal Ecology, Yerseke). Scheldt waters were found to be highly enriched in CH₄. Surface water saturation values ranged from about 15 times the atmospheric partial pressure in the coastal waters off Vlissingen (i.e. comparable to the concentrations around the 'Meetpost'), up to as much as 350 times saturation upstream of Antwerp. These findings indicate a relationship between dissolved CH₄ along the Dutch coast and freshwater input.

N₂O

In contrast to the variability in CH₄ concentrations, the surface water N₂O saturation was generally near equilibrium with the atmosphere, and tropospheric concentrations rather constant. Consequently the calculated water-atmosphere fluxes were small. These findings were confirmed by the results from the N₂O gradient measurements.

4 Discussion

Periodicity in the measured parameters.

During ASGASEX, sea water was pumped from an inlet at about 5 m depth and was analysed for several parameters, including CO₂, CH₄, N₂O, O₂, and temperature. Salinity was measured by 2 conductivity sensors mounted at about 5 and 7 metres depth. Most of the measured parameters showed a strong 12 hours periodicity (see figure). The origin of this periodicity is not yet clear (to me). As discussed before, this phenomenon may be explained by two hypotheses.

i) The 'vertical' hypothesis.

The water column was stratified around the depth of the water inlet (or gradients in the measured parameters had developed around this depth). The depth of the water inlet, with respect to the sea surface, changed periodically over an interval of about 2 metres under the influence of the tide (see figure). Consequently the origin of the sampled water varied over the concentration gradients of the various parameters in the water column, giving rise to the observed periodicity in the measured parameters.

ii) The 'horizontal' hypothesis.

The hydrographical situation around the 'Meetpost' is complex. Tide, (rest) stream, wind, and fresh water input of the Rhine, all influenced the water masses around the platform. The observed pattern in the measured parameters might be explained by a periodically returning type of water mass (Rhine plume?), driven by the tide.

Personally I (like to) believe in the 'horizontal hypothesis'. (note that I am rather subjective in this choice as the 'horizontal hypothesis' offers the most pleasant prospects for interpretation and publication of the CH₄ results)

Based on the enclosed figure of CH₄-tide-salinity-temperature for 17-18 September '93, I would like to make some remarks. Although these points are partly based on the CH₄ measurements, I expect they will be as much relevant for the CO₂, O₂ and N₂O data sets.

1) The figure shows that low tide, i.e. when 'shallow' water was pumped up, corresponds with high salinity. If the 'vertical hypothesis' is right, the high salinity layer must have laid ABOVE the less saline layer. This situation seems rather unusual (see also point 3). On the other hand, high salinity corresponds also with high temperature, having an opposite effect on the water density. Therefore water density should be plotted with tide to check whether a system with a warm and saline top layer could have been stable or not. (Note that the differences in both salinity and temperature were very small).

2) The figure shows that CH₄ corresponds with high salinity and high temperature. Based on the very high CH₄ concentrations which were measured in river water (see preliminary results), I would expect the opposite; namely high CH₄ corresponding with low salinity, i.e. with a high river water fraction. This is a second reason that makes the salinity record suspicious to me, which brings me to the following rather speculative point.

3) Might it be possible that there is something wrong with the salinity record? Some things could be better explained if the 'peaks' and 'valleys' in the salinity record would be interchanged (see remarks above). It might be wise to check the time basis of this data set. Salinity was measured with conductivity/resistance probes provided and mounted by 'Rijkswaterstaat'. Therefore it might also be wise to check whether the salinity record was calculated from a resistance or a conductivity data set? Mixing up of resistance and conductivity units might have resulted in a salinity record that differs by half a phase length, i.e. an interchange of the 'peaks' and 'valleys' in the signal.

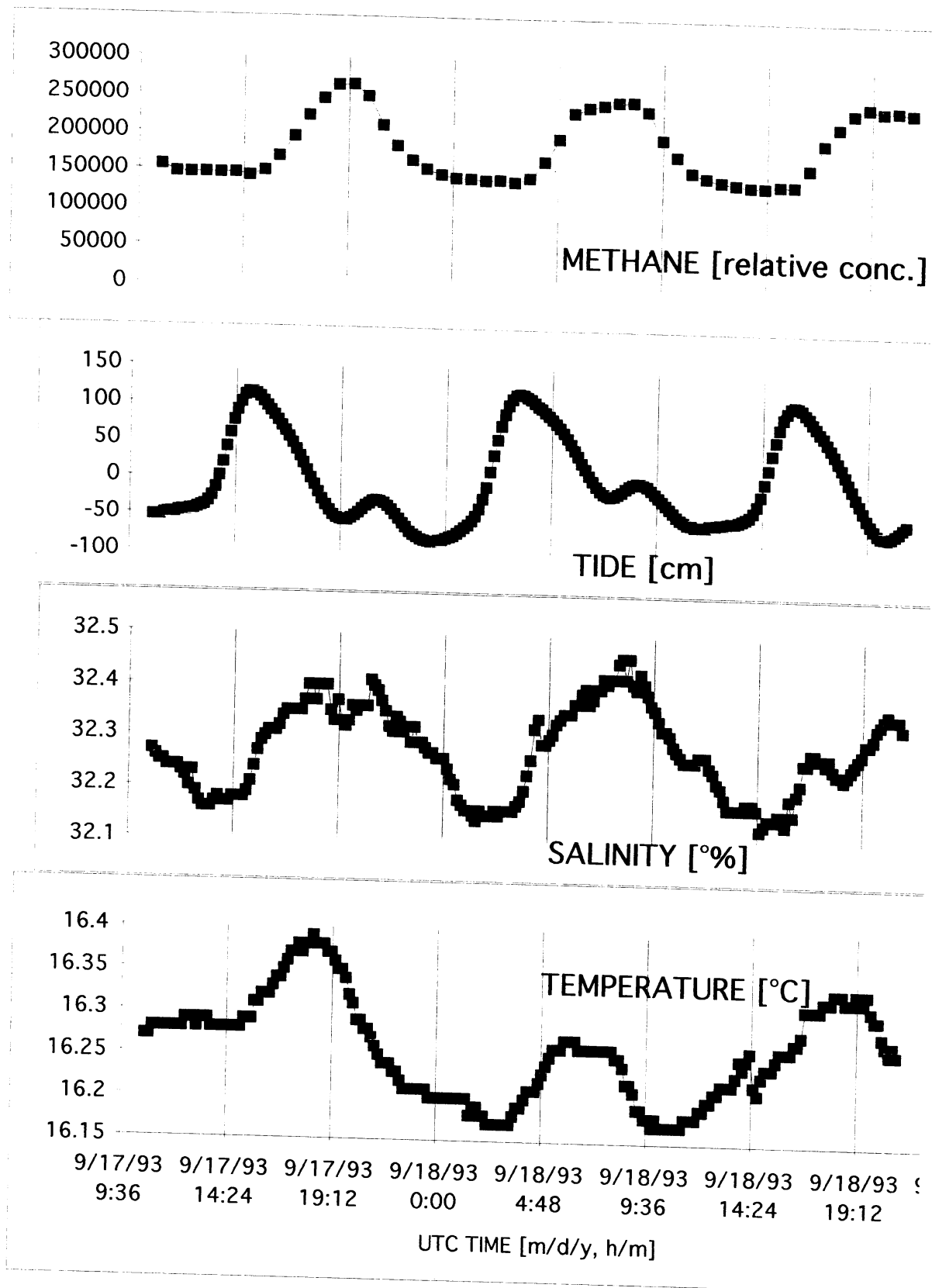
5 References

Badr O. and S.D. Probert (1993) Environmental Impacts of atmospheric nitrous oxide. *Applied Energy*, 44, 197-231.

Ericson D.J. (1988) Simulation of the global air-sea transfer velocity field of helium. *Geophysical Research Letters*, 15, 1495-1498.

- IPCC (International Panel on Climate Change) (1992), *Climate Change 1992*, the supplementary report to the IPCC Scientific Assessment. J.T. Houghton, B.A. Callander, and S.K. Varney, editors, Cambridge University Press, New York.
- Liss P.S. and L. Merlivat (1986) Air-sea gas exchange rates: introduction and synthesis. In: *The role of air-sea exchange in geochemical cycling*. P. Buat-Menard, editor, Reidel, Dordrecht, pp. 113-127.
- Oost W.A. (1994) The ASGASEX experiment. *KNMI Technical report TR-161*, pp 30, Royal Dutch Meteorological Institute (KNMI), De Bilt.
- Robertson J.E., Watson A.J., Langdon C., Ling R.D. and Wood J.W. (1992) Diurnal variation in surface pCO₂ and O₂ at 60 °N, 20 °W in the North Atlantic. *Deep Sea Research*, 40, 409-422.
- Wanninkhof R. (1992) Relationship between wind speed and gas exchange over the ocean. *Journal of Geophysical Research*, 97 (C series, 5): 7373-7382.
- Weiss R.F. and Price B.A. (1980) Nitrous oxide solubility in water and seawater. *Marine Chemistry*, 8, 347-359.
- Wiesenburg D.A. and Guinasso N.L. (1979) *Journal of Chemical and Engineering Data*, 24, 356-360.

Relationships between dissolved methane, tide, salinity and temperature at MPN during ASGASEX



CO₂ air-sea exchange from air-sea concentration differences in the Dutch coastal zone

D.C.E. Bakker, H.J.W. de Baar and A.A.J. Majoor
Netherlands Institute for Sea Research

Introduction

A discrepancy exists between CO₂ air-sea exchange from air-sea concentration differences and that from the eddy-correlation technique: a much discussed controversy (Smith and Jones, 1986; Broecker et al., 1986; Wesely, 1986). Fluxes from the eddy correlation technique tend to be a factor ten higher than those by the air-sea concentration gradient technique. Broecker et al. (1986) stressed that the detection limits of the eddy correlation technique were in the range of the expected air-sea exchange.

The ASGASEX (Air-Sea Gas Exchange) experiment was organised in September 1993 at Platform Noordwijk 9 km off the Dutch coast by Dr. W.A. Oost of the KNMI. Its major objective was to compare independent methods to estimate CO₂ air-sea exchange. The eddy correlation technique was applied by KNMI, FEL-TNO and BIO, while DAL and NIOZ determined air-sea exchange from the air-sea concentration difference. The atmospheric gradient technique was applied for methane by Ir. H.P.J. de Wilde of NIOZ.

Methods

Continuous measurements of the fugacity of carbon dioxide (fCO₂) in marine air and surface water, of total inorganic carbon (TCO₂), salinity and temperature were performed between 8 and 29 September 1993. Water was collected 5 m below average sea level with a submerged pump at high flow speeds. Average difference between the high and low water level was 1.6 m, the maximal difference 2.0 m. Total water depth was 18 m. Marine air was collected from the boom at 18.5 m above sea level.

Seawater was sprayed into an equilibrator built at NIOZ after the design of Dr. A.J. Watson for determination of fCO₂. The headspace of the equilibrator was sampled every 10 minutes by a gaschromatograph custom-built by Chrompack after Watson. Components of the gaseous sample were separated on two Hayesep D columns. CO₂ was converted to methane and burned at the FID-detector, which induced an electronic signal. Each GC-run included a sample for fCO₂ in air and water and three secondary standards, calibrated against four NOAA cylinders. The temperature of the water at the inlet and that in the equilibrator were registered. Temperature correction of Copin-Montégut (1988, 1989) was applied. Air-sea fluxes were calculated as the product of the concentration difference of dissolved CO₂ in water and air and a wind speed dependent transfer velocity with the relationship of Wanninkhof (1992).

For TCO₂ a volume of seawater was acidified, such that the inorganic carbon components evaded the solution as gaseous CO₂ and were determined by coulometry (Stoll, 1994).

Surface water methane (CH₄), laughing gas (N₂O) and oxygen (O₂) were detected by other participants on the same water supply. The platform's registration system acquired information on wind velocity, air temperature, atmospheric pressure, atmospheric moisture content, water height, current speed and - direction.

Results

Wind speed was low with short-lived maxima of 12 m·s⁻¹ at 10 and 21 September and a persistent spell of strong wind of 16 m·s⁻¹ at 25-26 September. Wave height was below 1.5 m, but increased to over 3.0 m at the 26th. Winds were easterly to southerly, except higher winds which were westerly, northerly to north-easterly. Most air had a terrestrial signature (east-northeast to south-southwest), but for strong winds. Major cities of the Netherlands (The Hague, Amsterdam, Rotterdam) and industrial areas (Rotterdam-Europoort, IJmuiden, industries along the North Sea Channel) were at close distance.

8-12 September

Surface water salinity and temperature were highly variable with the tide. Salinity was between 30.5 and 32.5, temperature between 16.6 and 17.0°C. fCO₂ in water varied from 320 to 380 µatm with the tide. It became 450 µatm with high salinity at the 12th. fCO₂ in air varied from 350 to 450 µatm with low south-easterly to north-westerly winds. Air-sea exchange was between -10 to 10 mmol·m⁻²·d⁻¹.

15 to 24 September

Water temperature, salinity, fCO₂ and TCO₂ varied with the tide. fCO₂ and TCO₂ were extremely variable. fCO₂ maxima upto 800 µatm were related to high salinity. This suggested water from the North Sea, possibly from below the mixed layer, enriched in inorganic carbon by mineralization. Atmospheric fCO₂ varied between 360 and 450 µatm. Air-sea exchange was generally between 0 to 20 mmol·m⁻²·d⁻¹ directed from the sea to the atmosphere with maxima upto 60 mmol·m⁻²·d⁻¹.

25 to 27 September

This period was marked by a persistent spell of strong wind upto 16 m·s⁻¹ at the 25th and 26th. Wave heights reached over 3.0 m. Water temperature and salinity were less variable with tide. Water temperature showed a steady decrease by autumn cooling. Surface water fCO₂ was undersaturated and relatively stable between 300 and 350 µatm. The undersaturation could have been caused by cooling of the water and an autumn bloom, stimulated by mixing. Atmospheric fCO₂ stabilised at 350 µatm. Air-sea exchange was generally between -10 and 0 mmol·m⁻²·d⁻¹, though it varied between -20 and 20 mmol·m⁻²·d⁻¹.

28 to 29 September

At the 28th an intrusion of less saline water with salinity 29 passed the platform. Apparently the effect of wind mixing of the 25th and 26th only lasted 3 days. The salinity minimum coincided with a change to supersaturated fCO₂ upto 400 µatm.

Atmospheric CO₂ remained stable. Air-sea exchange was generally between 0 and 10 mmol·m⁻²·d⁻¹.

Discussion

Careful study and cross checking of the hydrographic parameters (including oxygen, laughing gas and methane) are necessary get a grip on the hydrography. A strong salinity gradient may occur from the coast seaward due to river outflow (ICES, 1962). Even with low river outflow in September the salinity gradient may have been well expressed due to the persistently calm conditions. Large horizontal hydrographic variety and meandering of sloping local fronts may have been present. Stratification of the water column could not be excluded (de Ruijter, personal communication). The strong winds of the 25th and 26th would have mixed water to the bottom and over large distances.

Atmospheric fCO₂ values had been clearly influenced by antropogenic activities, when the air had passed over land.

CO₂ air-sea exchange from air-sea concentration differences was with a few exceptions within the detection limits for the eddy-correlation technique indicated by Broecker et al. (1986). Comparison of fluxes by the air-sea concentration difference and those by the eddy correlation technique showed the latter to be a factor ten higher than the former (Kunz et al., this issue), in accordance with the existing controversy (Smith and Jones, 1986; Broecker et al., 1986; Wesely, 1986). A reason for the discrepancy has not been identified yet.

Recommendations

It is necessary to optimise factors that promote the success of future intercomparisons of techniques to determine CO₂ air-sea exchange. Preferably experiments should take place with maximal and stable CO₂ fluxes. Timing of the experiment is very important. Intervals during which the actual intercomparison takes place, should be optimised and attention should be paid to the adjustment times of instruments, like equilibrators and sensors. Use of a LICOR for the detection of fCO₂ enhances the sampling rate and should be an improvement. Other locations might allow study of specific aspects of the exchange and of its registration by individual techniques. Here one could think of wind wave tanks or moderately sized lakes.

The conditions below promote steady and maximal fluxes at Platform Noordwijk. High wind speeds increase the transfer velocity and cause mixing of the water to the bottom and over large areas, but may cause technical and logistical difficulties. Winds originating from sea carry air with relatively stable fCO₂. Strong winds from sea tend to keep the river outflow in a narrow band along the coast. Low river discharge decreases heterogeneity of the coastal zone. Low marine biology is preferable as biology stimulates a patchy character of inorganic CO₂ in surface water. Continuous cooling or heating of the water promotes undersaturation respectively oversaturation of surface water fCO₂.

Acknowledgements

Ir. H.J.W. de Wilde was with us at the platform and work was performed in an atmosphere of joined co-operation. The research would not have been possible without the MPN crew and Rijkswaterstaat. Ing. F.A. Koning joined us with preparations and calibrated the gas cylinders. Ing. E. de Jong improved data-processing. Mr. M.W. Manuels helped with the salt calibrations, while Dr. H.M. van Aken processed them.

References

- Broecker, W.S., J.R. Ledwell, T. Takahashi, R. Weiss, L. Merlivat, L. Memery, T.H. Peng, B. Jähne and K.O. Munnich, 1986. Isotopic versus micrometeorological ocean CO₂ fluxes: a serious conflict. *Journal of Geophysical Research*, vol 91 (C9) p 10,517-10,527.
- Copin-Montégut, C., 1988. A new formula for the effect of temperature on the partial pressure of CO₂ in seawater. *Marine Chemistry*, vol 25, p 29-37.
- Copin-Montégut, C., 1989. Corrigendum. A new formula for the effect of temperature on the partial pressure of CO₂ in seawater. *Marine Chemistry*, vol 27, p143-144.
- ICES, 1962. Mean monthly temperature and salinity of the surface layer of the North Sea and adjacent waters. ICES, Charlottenlund.
- Kunz, G.J., G. de Leeuw, S.E. Larsen and F.A. Hansen, in preparation. Some preliminary results of TNO's micrometeorological observations during ASGASEX. In: Oost (ed.) Abstracts of the presentations during the ASGASEX workshop at KNMI, 3-5 October 1994. KNMI technical report.
- Smith, S.D. and E.P. Jones, 1986. Isotopic and micrometeorological ocean CO₂ fluxes: different time and space scale. *Journal of Geophysical Research*, vol 91 (C9), p 10,529-10,532.
- Stoll, M.H.C. 1994. Inorganic carbon behaviour in the North Atlantic Ocean. Thesis Rijksuniversiteit Groningen, Groningen. 193 p.
- Wanninkhof, R.H., 1992. Relationship between wind speed and gas exchange over the ocean. *Journal of Geophysical Research*, vol 97 (C5), p 7373-7382.
- Wesely, M.L., 1986. Response to "Isotopic versus micrometeorological ocean CO₂ fluxes: a serious conflict" by W. Broecker et al. *Journal of Geophysical Research*, vol 91 (C9), p 10,533-10,535.

Size distributions of bubbles and aerosols

Gerrit de Leeuw and Leo H. Cohen

TNO Physics and Electronics Laboratory

P.O. Box 96864, 2509 JG The Hague, The Netherlands

1. INTRODUCTION

The role of bubbles in air-sea gas transfer has been described in several publications (e.g., Thorpe [1982], Merlivat and Memery [1983], Woolf [1993]) and experimental evidence has been presented [Lamarre and Melville, 1991; Wallace and Wirick, 1992; Farmer et al., 1993]. To better understand the physics of air-sea exchange, bubble size distributions were measured by the TNO Physics and Electronics Laboratory (TNO-FEL) during ASGASEX, in combination with fluxes of CO₂ and profiles of aerosol size distributions. Bubble plumes were measured with sonar techniques by UCG and SUDO, as described elsewhere in this report.

The aerosol size distribution profiles were measured together with bubble size distributions to derive a quantitative source function for sea spray aerosol as function of meteorological and oceanographic parameters. The bubble-mediated production of sea spray aerosol has been studied for many years (e.g., Blanchard [1989]). New techniques are being explored to study the bubble bursting process and the subsequent production of jet droplets in great detail [Spiel, 1991; 1994]. The results can be used to formulate the oceanic source function, provided that oceanic bubble spectra are available for a wide range of conditions. However, this is not sufficient because sea spray aerosol droplets are also produced by direct tearing from the wave crests due to wind stress in high wind speeds ($u > 9$ m/s) [Monahan et al., 1986]. We feel that from the combination of realistic bubble-mediated jet droplet source functions derived from *in situ* bubble spectra, combined with simultaneously measured aerosol particle size distributions, the effects of direct tearing and bubble-mediated production can be separated. In that case, both production mechanisms can be evaluated as function of environmental parameters and combined into a consensus source function that applies in a wide range of conditions.

In this contribution we report on the bubble measuring system (BMS) that we developed and its deployment in open sea in studies on the air-sea exchange of gases and aerosols. The measurements of aerosol size distributions are described in brief. Flux measurements are described elsewhere in this report [Kunz and De Leeuw, 1994]. In section 2 we describe the BMS and the data processing, as well as the deployment from a float in open sea. In section 3 the aerosol measurements are described. An overview of the measurements and some preliminary results are presented in section 4. The results are discussed in section 5, which also gives the first conclusions. The bubble measurements were previously presented in De Leeuw and Cohen [1994].

2. THE BUBBLE MEASURING SYSTEM

A bubble measuring system (BMS) was developed and constructed by TNO-FEL. The sizes of single bubbles are measured in sea water to obtain bubble size distributions in the diameter range from 30 μm to 1000 μm . The BMS system is schematically shown in Figure 1. The sample volume is illuminated by a diode laser and viewed by a ccd camera via a telescope. The length of the sample volume is limited by the conical tubes in which windows and lenses are mounted. The lengths of these tubes have been chosen such that all bubbles inside the sample volume are in focus. The conical shape has been chosen to reduce the creation of turbulence near the sample volume.

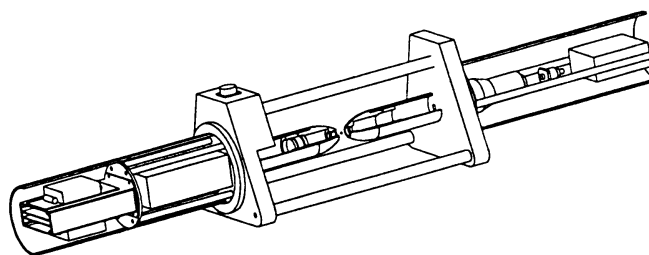


Fig. 1. The TNO-FEL bubble measuring system measures the sizes of single bubbles in the sample volume that is illuminated by the laser beam and imaged on the ccd camera through a telescope. The length of the sample volume is limited by the conical pipes in which the windows and lenses are mounted.

The camera signal is fed into a dedicated processing board for on-line analysis of the size and shape of objects in the sample volume. The processing assumes a spherical bubble shape and the aspect ratio is used as a selection criterion. Non-spherical shapes are assumed to be particles or biological species. The number of non-spherical shapes is retained in the data files. The images are also recorded on S-VHS video tape.

The BMS was calibrated with circles on paper which were photographically reduced to a known size. The smallest bubble size that we can presently measure is 60 μm , as compared to the aimed 30 μm . This smaller size could be measured by an optimized processing algorithm that will be developed for future applications, or by using a larger

magnification in the telescope (at the expense of the smaller sample volume).

During the ASGASEX campaign, power supply and data recording were located on the MPN and the BMS was deployed with a 100-m long cable to the tower. A self-contained system that telemeters the data to a receiving station ashore over a maximum distance of 10 NMi is also available.

During ASGASEX the BMS was deployed on a small float that consisted of a life-buoy and a pole extending 0.5-2 m (adjustable) below the surface. The BMS was mounted at the bottom of the pole. We deployed the BMS only at 0.5 m and at 1 m below the surface. The pole was mounted on gimbals to keep the BMS horizontal. The buoy was attached to the MPN tower with lines, at a distance of 50-100 m from the tower to reduce the influence of bubbles generated by (tidal) currents around the tower. Because the influence of the tidal current was still evident in the spectra, cf. Figure 2, a second float was anchored NW from the platform and used to keep the BMS out of the current-generated plume.

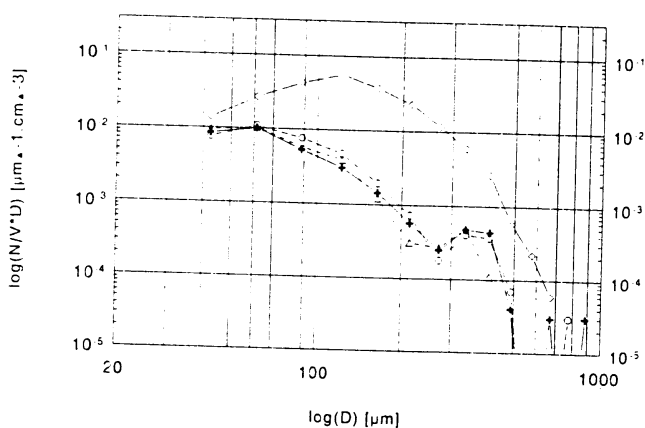


Figure 2. The influence of the bubble plume generated by the platform due to the tidal current is evident in the bubble size distributions shown in this Figure. The horizontal axis shows the bubble diameter in μm on a log scale, the vertical axis shows the number concentrations, per cm^3 , per size increment (in μm). The upper curve was measured in the bubble plume, the lower curves were measured outside the bubble plume. The number of bubbles in the plume is much larger, especially for the larger bubbles, which causes a shift of the median diameter to larger sizes. The data were collected at 0.5 m below the surface.

3. AEROSOL MEASUREMENTS

Aerosol particle size distributions were measured with two methods. An optical particle counter, a Particle Measuring Systems (PMS, Boulder, CO) CSAS 200 P that measures particles in the diameter range from 0.2-20 μm was mounted at the lower deck of MPN, at 11 m above the mean sea level. The optical particle counter was continuously operated and data were stored as 1-minute samples.

Profiles of particle size distributions were measured with Rotorod inertial impaction samplers mounted on the pulley and float system that was also used during previous experiments from MPN [De Leeuw, 1987, 1990]. The Rotorod samples particles larger than 12 μm in diameter. It consists of two polished stainless steel rods, mounted in a retracting collector head on a motor that rotates at a nominal speed of 2400 RPM. The linear velocity of the rods is 10 m/s. Particles impacted on the rods are retained by a sticky coating (silicone). Microscope images of the rods are digitized to determine the particle size distribution by computer. The profiles were measured at a distance of 13 m from the platform by using a horizontal mast extending north from the NW corner of the platform. Flow distortion by the platform structure, and the influence of waves breaking on the platform, are negligible at this position. The Rotorod samplers were mounted on a rod that slid along a vertical line extending from the tip of the mast down into the water. The measurements were made from just above the wave tops up to about 15 m. Wave following measurements were made with the Rotorods attached to a float, at 0.2 m to 3 m above the instantaneous water level.

4. RESULTS

a. Bubble size distributions

During the ASGASEX experiments, bubble size distributions were measured as 15-minute averages, in images recorded on video tape. Altogether about 36 hours were recorded, which translates into about 144 samples. The initial recordings, where the influence of the platform was evident, were deleted from the data set. Due to several other problems, also many of the images recorded later-on were not reliable and had to be deleted from the data set. After thorough validation, based on spectral shape and bubble concentrations, only 40 reliable bubble size distributions were left for further analysis.

In Figure 3 we present a comparison of one of these bubble size distributions with spectra presented in the literature. The fairly good agreement with the literature data gives confidence in our system.

A second test is the variation of the bubble concentrations with environmental parameters. Trends were observed that indicate a dependence of the bubble concentrations on fetch and wind speed. These are discussed below. Unfortunately, statistical relations cannot be derived because the data set is too small for a detailed analysis based on the subdivision for, e.g., a range of fetches or wind speeds (cf. Van Eijk and De Leeuw [1992] for an example of such an analysis of aerosol particle size distributions at MPN).

In the time series in Figure 4 we discern seven longer periods. For each period the observations are briefly described, including the meteorological characterization. We note that until 15 September the BMS was deployed at 0.5 m below the instantaneous water surface, and from 26 September the depth of the BMS was 1 m. The variation of the bubble concentrations with depth has been reported in the literature (e.g., Wu [1992]), but the present data base does not allow for such an analysis.

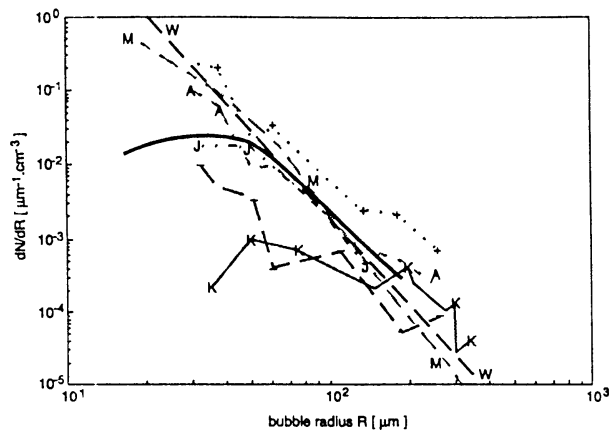


Figure 3. Comparison of bubble size distributions measured with our BMS. with spectra presented in the literature. All spectra were measured in a wind speed of 13 m/s. Other environmental parameters were different, however, as were the depths at which the data were collected and the techniques that were used. Note that bubble size is presented by the radius in μm , and therefore also the concentrations are given in number of bubbles per cm^3 per μm radius increment. The spectrum labelled K is from Kolovayev [1976], J is from Johnson and Cooke [1979], M is from Monahan [1988], W is from Wu [1989] and +, - and A are spectra from Medwin and Breitz [1989] just after wave breaking, the average and the minimum concentrations, respectively.

On September 10, 08:47-19:21, we have 6 spectra, over a total period of 10.5 hours. During this period the wind was from the south west, decreasing from 14.3 m/s to about 12 m/s. Significant wave height was 1.4 m. The thermal stratification was neutral to slightly unstable (air-sea temperature difference, or ASTD, was -0.5°C to -0.9°C). On average, the concentrations of the larger bubbles decrease, as expected. However, the concentrations of the smaller bubbles only initially decrease and then increase slightly. The latter observations are not yet understood. However, instead of wind speed, the effect of wind stress (or the drag coefficient) should be considered because these parameters describe wave breaking, and thus bubble formation, better than wind speed alone. Stress is also influenced by fetch, surface current, the angle between wind and waves. etc.

On September 13, 08:26-17:06, seven validated spectra are available spread over a period of 8.5 hours. The wind was from ESE, about 9.5 m/s. Significant wave height was 0.7 m. The thermal stratification was unstable, with ASTD -2.4°C . The bubble concentrations were fairly constant during this period, although more variation is observed in the concentrations of the larger bubbles than for the smaller ones. However, in spite of the lower wind speed as compared with the previous period on September 10, the bubble concentrations on September 13 are about a factor of two higher than on September 10, for all sizes. This effect is more pronounced for the smaller bubbles.

The increase in the concentrations is presumed to be due to the effect of fetch. The fetch in this ESE wind is much shorter than in SW winds. This results in younger waves which are steeper, resulting in more breaking. To verify these arguments, and to quantitatively describe the observed phenomena, data are required on stress and on whitecap recordings. Because the sonic anemometers were mounted on the west side of the MPN, i.e. in the wind shadow, direct measurements of the stress were not made. Whitecap data were not available at the time of writing this contribution.

On the next day, September 14, 5 validated bubble size distributions are available for an 8 hour period, 09:42-17:27. The conditions were similar to the previous day, although the wind speed was somewhat lower and decreased further (from 8.4 to 6.2 m/s). Wind direction was ESE, waves decreased from 0.8 m to 0.6 m. The thermal stratification was unstable with ASTD increasing from -4°C to -2°C . The bubble concentrations are seen to decrease only slightly, although for the larger bubbles the concentrations are very variable and no clear trend is observed.

On 26 September we have only three validated spectra over a four hour period between 15:38 and 19:20. Nevertheless this period is interesting because of the high wind speed of around 18 m/s, from the NE, with waves increasing from 3 to 3.4 m/s. Thermal stratification was unstable, with ASTD -3.1°C . The concentrations of the smaller bubbles ($\mu 214 \mu\text{m}$) are clearly higher (by about a factor of 2) than in any of the previous periods. For the larger bubbles, however, there are little or no data. This might be due to the deeper deployment of the BMS (-1 m as compared to -0.5 m during the previous periods), but this is not likely because in this high wind speed deeper mixing would be expected. Wave age might be another consideration, but presently we cannot explain the observations (or better the lack of observations) for the larger bubbles.

On the following day, September 27, the wind still was from northerly directions, but the wind speed had decreased significantly to 3-5 m/s. Waves were still high and decreasing from 1.7 m to 1.3 m. The ASTD increased from -1.6°C to -0.6°C . Four bubble spectra are available for a period of 3.5 hours between 06:06 and 09:25. The bubble concentrations were fairly constant, decreasing for the larger sizes. As expected, the concentrations were appreciably lower than during the preceding high wind period, and, except for the smallest bubbles, also lower than in other periods discussed thus far. This is explained by the weak winds and the long fetch, in which no significant whitecapping is expected.

On September 28, 06:10-21:52, we have 6 bubble size distributions over a 16 hour period, with a 10 hour interruption after the first two measurements. The wind was SSW, 8 m/s in the morning while in the evening series the wind speed started at 12.4 m/s, decreasing to 10 m/s. Significant wave heights were about 0.8 m.

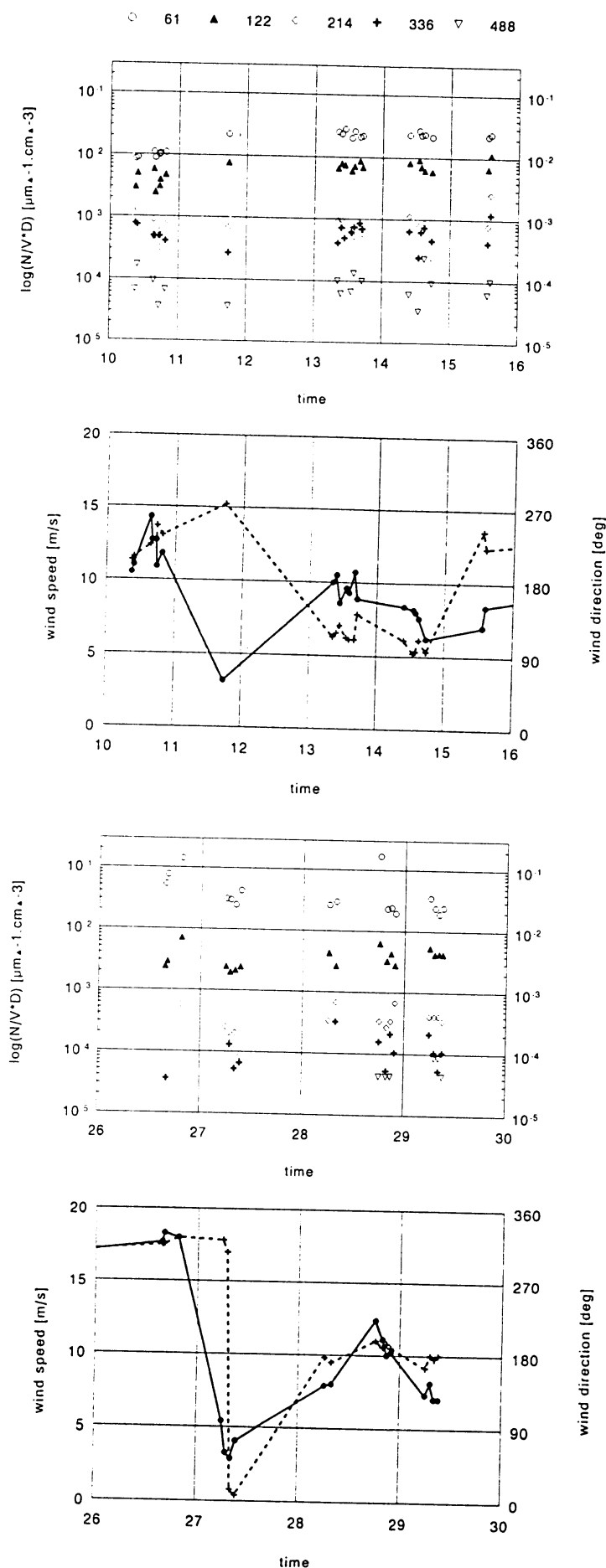


Fig. 4. Time series of bubble concentrations, for bubbles with diameters of 61 μm , 122 μm , 214 μm , 336 and 488 μm (see legend at the top), and wind speeds (solid line) and wind directions (broken line) during the measurements. The connecting lines in the wind data are not extrapolations. Note that the concentrations are given as number of bubbles per cm^3 per μm diameter increment. The upper two panels present the data for the first period from 10 to 16 September, the lower two panels are for the period 26 to 30 September. The numbers on the horizontal axes indicate the day in September.

The atmosphere was unstable, with ASTD -3.7°C in the morning and -2.7°C in the evening. The higher wind speed of 12.4 m/s at the start of the evening measurements resulted in a peak in the bubble concentrations for the smaller sizes, but not for the larger ones. In general, the concentrations were actually observed to decrease somewhat.

Presently we have no explanation for the latter observation. May be mixing processes are an issue both here and in the observations regarding the concentrations of the larger bubbles on the previous day, but at this moment we can only present speculations which are not supported by experimental data or models.

On September 29, 06:07-09:08, 4 bubble size distributions are available over a period of three hours. Wind speed was 7-8 m/s, from the south. Significant wave height was only 0.5 m and ASTD was -4.3°C , i.e. very unstable. The bubble concentrations are observed to decrease slightly, more for the larger bubbles than for the smaller ones.

b. Aerosol measurements

During ASGASEX eight profiles of particle size distributions were measured with the Rotorod inertial impaction samplers. These will be analyzed together with the eighteen profiles that were measured during the MAPTIP trial that was conducted from MPN immediately after ASGASEX [Van Eijk et al., 1994]. MAPTIP was focused on aerosols. An initial analysis of the ASGASEX/MAPTIP profile data base was presented in Davidson et al. [1995].

The optical particle counters were continuously operated. However, the wind directions during ASGASEX were predominantly easterly in which the particle counters were shielded by the platform. Hence the aerosol data are only reliable and representative for open sea conditions in winds with westerly components (wind directions 110° to 340° with respect to North). To obtain a statistically significant amount of data, also the aerosol size distributions measured with the optical particle counters are combined with the MAPTIP data. A preliminary analysis of the MAPTIP data set was presented in Van Eijk et al. [1995]. The primary objectives of these analyses was the validation of the MPN model, that is based on data collected during the HEXMAX experiments [Van Eijk and De Leeuw, 1992], the extension of the MPN model to a wider range of conditions and the generalization of the MPN model to other parts of the North Sea.

5. DISCUSSION AND CONCLUSIONS

In the above data presentation we have indicated trends in the bubble concentrations and the evolution of the bubble size distribution with environmental parameters. Wave breaking, and thus also the bubble concentrations resulting from the wave breaking process, are determined by wind speed and other parameters such as surface currents and fetch. Together these parameters also determine the wind stress. Unfortunately the stress could often not be directly measured during ASGASEX because all equipment had been mounted at the west side of the MPN, while during ASGASEX the winds came predominantly from easterly directions. Thus the instruments were sheltered by the MPN and reliable data could not be obtained during most of the time.

Direct measurements of the whitecapping ratio, the surface manifestation of the emerging bubble plume, were not available at the time of writing this contribution. Therefore we have thus far described our observations only in terms of the available bulk meteorological parameters such as wind speed, wind direction, significant wave height and ASTD. Another factor to consider is the surface current caused by tidal effects, and the effect of river outflows on the salinity and the surface roughness. Also biological effects should not be forgotten in this coastal North Sea area. Especially because these may also create bubbles.

Our validated data base turns out to be too small to separate and quantify individual effects on the bubble size distribution. The observation of large bubble concentrations in relatively short fetch is ascribed to the enhanced breaking of young waves that are steeper than in a well-developed wave field

The results have not yet been interpreted in terms of air-sea gas exchange and the production of sea spray aerosol. This requires a modeling effort which we hope to pursue in the future.

The aerosol data collection was continued during the MAPTIP campaign that was conducted from the MPN in October-November 1993 [Van Eijk et al., 1993]. The ASGASEX and MAPTIP aerosol data are analyzed as one (semi-) continuous data base. These data are used to validate the MPN aerosol model that resulted from the HEXMAX data base [Van Eijk and De Leeuw, 1992], to extent this model to easterly wind directions, and to further analyze the height dependence of the aerosol size distributions. An initial attempt will be made to derive an aerosol source function for the area.

The deployment of the BMS during the ASGASEX campaign was a first test in open sea, and also the first deployment during an extended period of time. These initial tests have indicated that some improvements to the BMS are required, especially as regards the hard ware. The recordings show that the North Sea water contain many particles and organisms of biological origin. Our BMS cannot discriminate between spherical particles and bubbles. This might be a reason for the relatively large number of bubbles counted at low wind speeds, and the relatively small

sensitivity of the bubble concentrations to changes in wind speed. This asks for a detailed analysis of the recorded tapes for selected periods. If indeed many spherical shapes are counted which are not bubbles, a more sophisticated processing algorithm must be developed to discriminate between bubbles and other organisms and particles.

We feel that the bubble measuring system we developed is a useful contribution to the rare studies that are being made on bubble size distributions. The bubble concentrations and size distributions are similar to those obtained from other studies. Variations in the bubble concentrations have been explained by variations in environmental conditions. The data base is presently too small to derive quantitative relations between bubble size distributions and environmental parameters in a complicated environment such as the coastal North Sea.

ACKNOWLEDGMENTS

The bubble measuring system was developed with support from the TNO Central Organisation and the Netherlands Ministry of Defence (assignment A92KM714). The ASGASEX measurements were supported by EC DG XII (contract MAS2-CT93-0056) and the Netherlands Ministry of Defence (assignment A93KM635). We are grateful for the support of our colleagues at TNO-FEL during the ASGASEX campaign, and in particular we thank our colleagues from the 'Electronic Systems' division who built the BMS and developed the software.

REFERENCES

- Blanchard, D.C. (1989). The size and height to which jet drops are ejected from bursting bubbles in sea water. *J. Geophys. Res.* 94, 10999-11002.
- Davidson, K.L., P.A. Frederickson and G. de Leeuw (1995). Surface layer turbulence and aerosol profiles during MAPTIP. AGARD electromagnetic wave propagation panel 55th specialists' meeting on "Propagation assessment in coastal environments", Bremerhaven, Germany, 19-23 September, 1994. AGARD CP 567, paper 25.
- De Leeuw, G. (1987). Near-surface particle-size-distribution profiles over the North Sea. *J. Geophys. Res.* 92 (C13), 14631-14635.
- De Leeuw, G. (1990). Profiling of aerosol concentrations, particle size distributions and relative humidity in the atmospheric surface layer over the North Sea. *Tellus* 42B, 342-354.
- De Leeuw, G. and L.H. Cohen (1994). Measurements of oceanic bubble size distributions. OCEANS94, 13-16 September 1994, Brest, France. in press.
- Farmer, D.M., C.L. McNeil and B.D. Johnson (1993). Evidence for the importance of bubbles in increasing air-sea gas flux. *Nature* 361, 620-623.
- Johnson, B.D., and R.C. Cooke (1979). Bubble populations and spectra in coastal waters: A photographic approach. *J. Geophys. Res.* 84, 3761-3766.
- Kolovayev, P.A. (1976). Investigation of the concentration and statistical size layer distribution of wind-produced bubbles in the near-surface ocean. *Oceanology* 15, 659-661.

- Kunz, G.J., G. de Leeuw, S.E. Larsen and F. Aa. Hansen (1994). Eddy correlation fluxes of momentum, heat water vapor and CO₂ during ASGASEX. This report.
- Lamarre, E. and W.K. Melville (1991). Air entrainment and dissipation in breaking waves, *Nature* 351, 469-472.
- Medwin, H. and N.D. Breitz (1989). Ambient and transient bubble spectral densities in quiescent seas and under spilling breakers. *J. Geophys. Res.* 94, 12751-12759.
- Merlivat, L. and L. Memery (1983). Gas exchange across an air-water interface: experimental results and modeling of bubble contribution to gas transfer, *J. Geophys. Res.* 88, 707-724.
- Monahan, E.C. (1988). From the laboratory tank to the global ocean. In: *Climate and health implication of bubble-mediated sea-air exchange*, E.C. Monahan and Van Patten, Eds., Conn. Sea grant College Program, CT-SG-89-06, pp. 43-63.
- Monahan, E.C., D.E. Spiel and K.L. Davidson (1986). A model of marine aerosol generation via whitecaps and wave disruption. In: *Oceanic Whitecaps and their role in air-sea exchange processes*, E.C. Monahan and G. Mac Niocaill, Eds., Dordrecht, D. Reidel, pp. 167-174.
- Spiel, D.E. (1991). Acoustical measurements of air bubbles bursting at a water surface: bursting bubbles as Helmholtz resonators. *J. Geophys. Res.* 97, 11443-11452.
- Spiel, D.E. (1994). The number and size of jet drops produced by air bubbles bursting on a fresh water surface., *J. Geophys. Res.*, in press.
- Thorpe, S.A. (1982). On the clouds of bubbles formed by breaking wind-waves in deep water, and their role in air-sea gas transfer. *Phil. Trans. R. Soc. Lond.* A304, 155-210.
- Van Eijk, A.M.J., and G. de Leeuw (1992). Modeling aerosol particle size distributions over the North Sea. *J. Geophys. Res.* 97, 14417-14429.
- Van Eijk, A.M.J., D.R. Jensen and G. de Leeuw (1994). MAPTIP experiment, Marine Aerosol Properties and Thermal Imager Performance. In: *Atmospheric Propagation and Remote Sensing III*, W.A. Flood and W.B. Miller, Eds., in press.
- Van Eijk, A.M.J., F.H. Bastin, F.P. Neele, G. de Leeuw and J. Injuk (1995). Characterisation of atmospheric properties during MAPTIP. AGARD electromagnetic wave propagation panel 55th specialists' meeting on "Propagation assessment in coastal environments", Bremerhaven, Germany, 19-23 September, 1994. AGARD CP 567, paper 19.
- Wallace, D.R., and C.D. Wirick (1992). Large air-sea gas fluxes associated with breaking waves, *Nature* 356, 694-696.
- Woolf, D.K. (1993). Bubbles and the air-sea transfer velocity of gases. *Atmosphere-Ocean* 31, 517-540.
- Wu, J. (1989). Contributions of film and jet drops to marine aerosols produced at the sea surface. *Tellus* 41B, 469-473.
- Wu, J. (1992). Individual characteristics of whitecaps and volumetric description of bubbles. *IEEE J. of Oceanic Eng.* 17, 150-158.

Bubbles and vertical transport below the sea surface

by

David K Woolf

Department of Oceanography

University of Southampton

Highfield, Southampton

United Kingdom

Traditionally, a gas transfer flux, F , is related to the air-sea concentration difference, ΔC , by

$$F = K_T \Delta C$$

where K_T which has the dimensions of velocity is termed the air-sea transfer velocity or piston velocity. Taking account of the role of bubbles, in which case there are "direct" and "bubble-mediated" pathways of gas exchange, a gas flux equation

$$F = (K_O + K_b) [C_w - S p_a (1 + \Delta)]$$

is more appropriate, where K_b and Δ are associated with the inclusion of bubbles, while K_O is only the result of transfer directly through the sea surface (Woolf and Thorpe, 1991; Woolf, 1993).

The "supersaturation term", Δ , originates largely in the hydrostatic pressure on the bubbles and thus is highly sensitive to the depth to which bubbles are drawn by advection and dispersion in the upper ocean. The "gross enhancement" of bubbles to gas transfer, K_b , depends on the surface flux of bubbles and the lifetime of those bubbles. It is a difficult task to estimate the surface flux of bubbles. It is necessary to have detailed measurements of near-surface turbulence in addition to measurements of bubble concentration. Observations of vertical transport must accompany simple measurements of bubble concentration.

In addition, a vertical eddy diffusion coefficient can be deduced from the vertical distribution of bubbles (though one must ignore some distinctly non-Fickian aspects of the dispersion). Thorpe (1984) found that typically an eddy diffusion constant of $200 \text{ cm}^2/\text{s}$ best described the vertical attenuation of bubble clouds. The concentration difference in a gas at steady state across a layer of several metres depth with this level of mixing is fairly negligible compared to the expected concentration difference across the marine microlayer. The vertical penetration of bubble clouds during ASGASEX is well-documented with over 160 hours of data from the upward looking sonar on the IOSDL quadruped. This is a fine beam instrument operating at 4Hz and gives high resolution information on bubble distributions both at several metres depth and (at least when the waves are large) at levels between wave crest and wave trough. One of the observations is that patches of water "tagged" by bubbles can be advected down several metres in only a minute or so. Gas concentrations will only respond to air-sea fluxes relatively slowly (\sim days). In summary, it seems safe to regard water up to the maximum penetration depth of clouds (within the preceding ten minutes, say) as being "well-mixed" in respect to our interest in gas concentrations and fluxes. We have made a preliminary survey of "maximum bubble cloud depth" which may also be considered the "minimum surface mixed layer depth" over much of ASGASEX. Maximum cloud depth is plotted along with wind speed in the two figures (Figure 1, September 6-13; Figure 2, September 20-29). The cloud depth responds primarily but not solely to wind speed. It is likely that tidal current and pre-existing stratification also influence cloud depth. A thorough analysis of the dependence of cloud characteristics on environmental conditions is planned.

REFERENCES

- Thorpe, S.A. 1984. A model of the turbulent diffusion of bubbles below the sea surface. *J. Phys. Oceanogr.*, 14, 841-854.
- Woolf, D.K. 1993. Bubbles and the air-sea transfer velocity of gases, *Atmosphere-Ocean*, 31, 517-540.
- Woolf, D.K. and S.A. Thorpe. 1991. Bubbles and the air-sea exchange of gases in near-saturation conditions, *J. Mar. Res.*, 49, 435-466.

ASGASEX 93, wind speeds and cloud depths

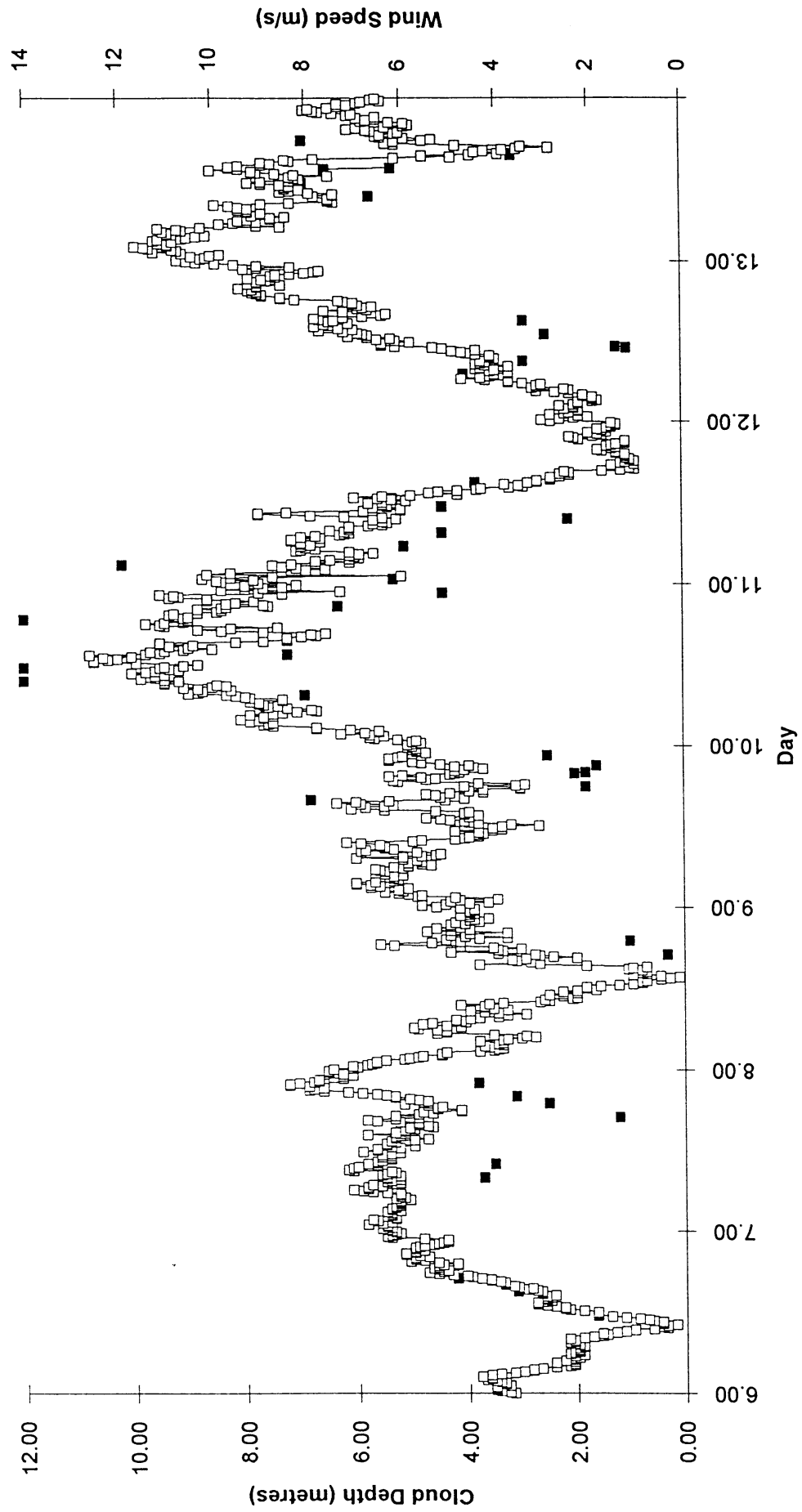


Fig.1

ASGASEX 93, wind speeds and cloud depths

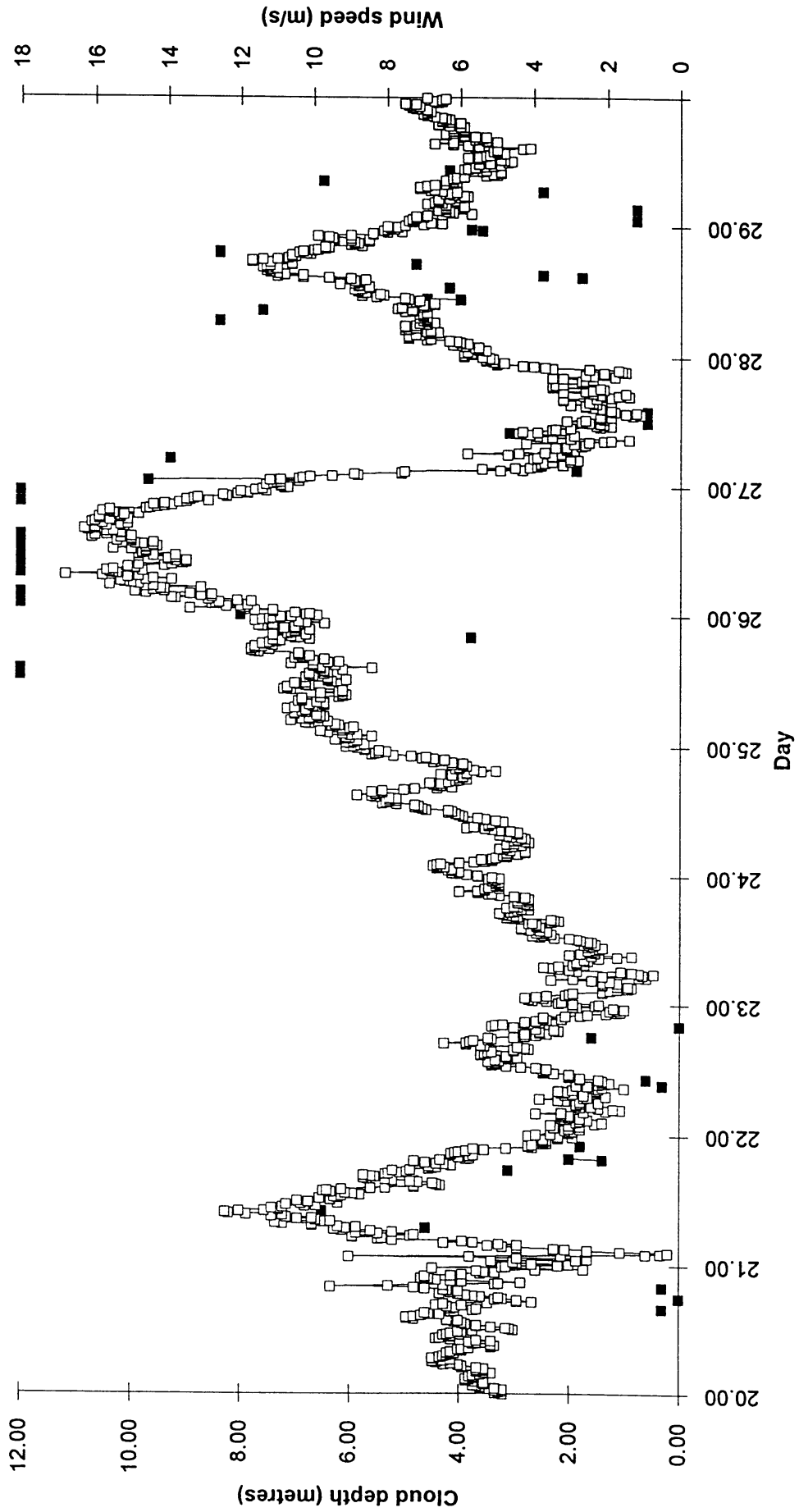


Fig.2

W.A. Oost (KNMI):
Trying to make it make sense.

Introduction

The central problem addressed in ASGASEX is the discrepancy between the value of the transfer velocity derived with the eddy correlation technique and existing parametrizations, such as those of Liss and Merlivat (1986) and Wanninkhof (1992). In this paper we will primarily use flux data measured by KNMI and CO₂ concentration data measured by NIOZ, as well as the 10m operational wind speeds from MPN to try to find out whether we can find some clues.

The KNMI flux data, used in our calculations, were measured with a Kaijo Denki sonic anemometer and the KNMI Infrared Fluctuation Meter (Kohsiek, 1991), both mounted at the end of the MPN instrument boom. The uncertainties in the flux data are substantial, due to the limited accuracy of the CO₂ sensor and the need to apply the so-called Webb correction (Webb et al, 1980), which over sea is comparable to or sometimes even bigger than the initial flux signal.

The water samples for which NIOZ determined pCO₂, were brought up with a submerged pump, mounted at a fixed position on one of the hydro-sensor poles of MPN. The average depth of the pump inlet was 5m, but due to the tide this value fluctuated between roughly 4 and 6m. The water from the pump was put through an equilibrator, and the equilibrated air was analyzed with a gas-chromatograph. The CO₂ concentration of the air (CO_{2a}) was measured directly with the same gas-chromatograph using air that had been sampled at the tip of the instrument boom.

The problem

After analyzing our ASGASEX data for the CO₂ flux, we plotted our results against the DpCO₂ (=pCO₂ - CO_{2a}) values found by NIOZ, assuming that the flux Φ was related to DpCO₂ according to the usual relationship

$$\Phi = k \times \text{DpCO}_2 \quad (1)$$

with k the transfer velocity.

The result, shown in fig.1, was a disaster: no systematic relationship and even the sign of both the flux and DpCO₂ changes haphazardly. Most of the data give values for k far in excess of the Liss-Merlivat or Wanninkhof parametrizations, except for run 64, one of the two points in fig.1 with DpCO₂ around 140 μ atm (for the other point the flux value had to be discarded due to flow distortion).

The off-hand conclusion, our flux data were only amplified noise, was contradicted by the fact that they showed a rather systematic behavior when plotted as a function of the wind speed (fig.2). We tried to use that behavior to eliminate effects due to the wind speed dependence of k , by reducing our flux data to wind speed zero, hoping still to find an acceptable relationship with DpCO₂, but again to no avail.

The rather high and fluctuating values of DpCO₂ then drew our attention. They are due to rather anomalous pCO₂ values from the water near MPN, the values for the air are quite normal and stable. After low-pass filtering of pCO₂ by applying a two hour running average we found a clear relationship with the tide (fig.3). This relationship is not always present and at least one of the factors affecting it is the wind speed: the tide-related fluctuations are mainly visible at low (<5 m/s) or decreasing wind speeds.

The obvious explanation for these fluctuations is that they are due to advection: the MPN platform is about 35km from the outflow of the river Rhine, a source of organic material in watery solution. There are, however, factors that raise doubts in this respect:

- Current measurements show that pCO₂ rises when the tidal current is southward, whereas the residual current in the southern North Sea is northward. It doesn't stand to reason that the high pCO₂ water should first be advected unnoticed past the platform, each time to be detected only when it returns in the next part of a tidal cycle.

- To explain the continuous change of pCO₂ by advection of bubbles of Rhine water, we are forced to assume that we are permanently in an area of concentration *gradients* in the water, without reaching a plateau or a reverse trend as long as we are in the same quart of the tidal cycle.
- We found no indication for advection of accompanying salinity changes; that quantity shows only small fluctuations during the measurement period. Only at the very end of ASGASEX, after the pCO₂ measurements had been finished, we detected a clear example of advection of water with a significantly lower salinity than measured during the rest of the period.
- That fresh water bubbles can maintain their identity in a way that causes the large fluctuations in fig.3 is also somewhat improbable: the distance to the mouth of the Rhine is 35km, whereas half a tidal period covers less than 10km. Reaching the platform from the mouth of the Rhine therefore requires a number of tidal cycles in fairly shallow water, with the consequent mixing of water masses.

As a consequence we would furthermore have to accept that (1) is not valid, due to high variability, despite the rather decent behavior of Φ in fig.2.

To get more information, again independent from the uncertain flux values, we also plotted pCO₂ as a function of the wind speed for the period September 20-29 in fig.4. It shows the rather unexpected feature of a wind speed dependent maximum value of pCO₂ (We could have plotted the same picture for the whole ASGASEX period, but that would have contained more dubious values). Figure 4 suggests a strong (note the range of pCO₂!) effect of an atmospheric quantity, the local wind speed, on pCO₂, a quantity representative for the situation at an average depth of 5m under water. Wind and tidal current are mutually independent, so the consequence of fig.4 appears to be that we have to envisage the possibility of local processes (local in both time and space) affecting the transfer process.

A solution ...?

We shall indicate the effect of fig.4 loosely as the "wind effect", 'This indication is chosen because we see a correlation with the wind, but is not intended to suggest anything about the mechanism behind it.

In view of the time scales and masses involved it is not possible that the wind should affect the whole of the 18m deep water column, or, in other words, deeper down the effect is absent or negligible. This again would entail that there is a local vertical concentration gradient. Fig.3 then may have a different explanation: the pCO₂ changes with the tide may have been - at the least: partially - local. This not only supports the idea of a vertical concentration gradient, but it also takes care of the problems met in ascribing the concentration changes purely to advective processes.

A trivial thought furthermore is that there is no wind effect if there is no wind, so at wind speed zero we may recoup the original concentration, without the wind effect. In fig.5 we plotted DpCO₂ (which, as can be seen, shows approximately the same behavior as pCO₂) and constructed a line that corresponded as well as possible to the wind dependent upper limit of the DpCO₂ values. This line crossed the y-axis of the figure at a value of 272 μ atm (we made no attempts at this exploratory stage to try to determine the accuracy of this number). If the wind effect is limited to a top layer of the water, with a thickness of a number of meters, we might find the original concentration again below this "wind" affected layer.

Assuming that pCO₂ at this deeper level was relatively constant during the relevant period, i.e. September 20-29, we calculated the CO₂ fluxes with (1) using DpCO₂ = 272 μ atm and values for k according to Wanninkhof (1992). The result, plotted in fig.6, is not unsatisfactory, certainly not in view of the uncertainties involved. FEL-TNO also made CO₂ flux measurements, which were completely independent of those of KNMI, but their results too show a good correspondence with the "RW272" curve (fig.7).

The first question, of course, now is whether these heretic ideas are even remotely true. This cannot be decided without further experiments, which we hope to be able to do in 1996 during ASGAMAGE, when we will try to make simultaneous pCO₂ measurements at two levels. Assuming for the moment that there is at least some truth in them, we can take another look at the controversy mentioned in the Introduction. Even if the "wind effect" should be limited to shallow water situations and be of no importance for oceanic conditions, than we can at least explain the large k values resulting from earlier eddy correlation experiments: the flux values were probably in general correct (i.e. unbiased, but with a large experimental uncertainty), but the DpCO₂ values were too small due to the "wind effect", as in fig.1. This applies to all eddy correlation measurements, because they require a stable platform, so all experiments to measure the CO₂ flux over the sea directly were made over shallow water or at the coast.

The solution of the problem - if true at all - is not a complete one. Fig.5 shows negative values of DpCO₂, whereas the "RW272" curve and most fluxes measured by KNMI were positive. Even if we assume that the deep concentration is driving the flux, we still have to explain how the CO₂ can get across the sea surface under these conditions. There is furthermore a phase shift between the tidal height and pCO₂ in fig.3 that has to be explained. And, of course: what is the mechanism behind the "wind effect"? We hope the 1996 ASGAMAGE experiments will bring some of the answers; we consider the ASGASEX material as sufficiently interesting to look further into the idea of a local vertical CO₂ gradient.

REFERENCES

- Kohsiek, W., 1991: Infrared H₂O/CO₂ sensor with fiber optics. *7th AMS symposium on Meteorological Observations and Instrumentation*, New Orleans, USA, Januari 13-18.
- Liss, P.S. and Merlivat, L., 1986: Air-sea gas exchange rates: Introduction and synthesis. In: P. Buat-Menard (ed.), *The role of air-sea exchange in geochemical cycling*, 113-127.
- Wanninkhof, R., 1992: Relationship between wind speed and gas exchange over the ocean, *J. Geophys. Res.* **97**, 7373-7382.
- Webb, E.K., Pearman, G.I. and Leuning, R., 1980: Correction of flux measurements for density effects due to heat and water vapour transfer. *Quart. J. Met. Soc.* **106**, 85-100.

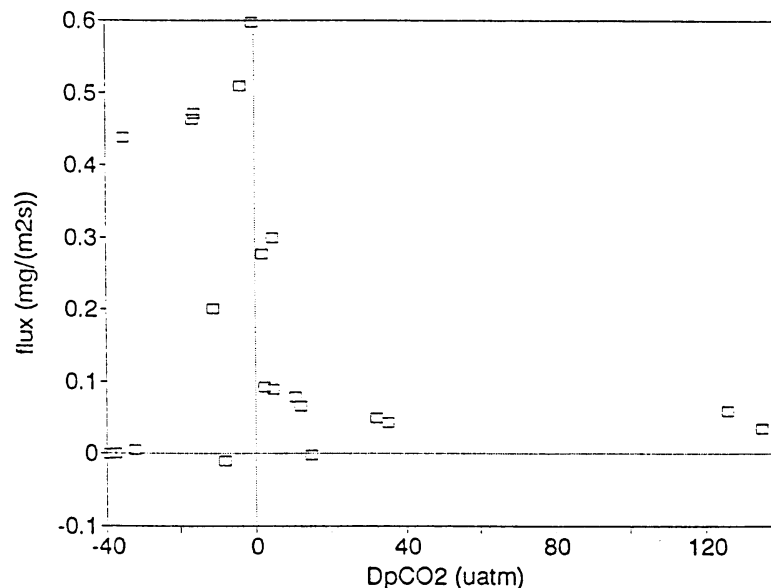


Fig.1 CO₂ fluxes measured with the KNMI Kaijo Denki/IFM combination as a function of the CO₂ concentration difference DpCO₂.

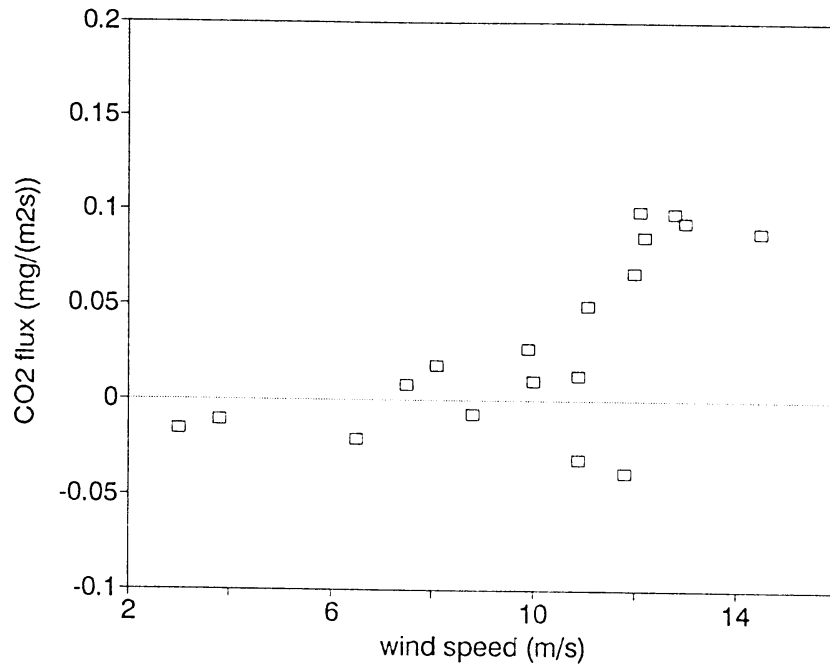


Fig.2 The CO₂ fluxes of fig.1 as a function of the 10m wind speed.

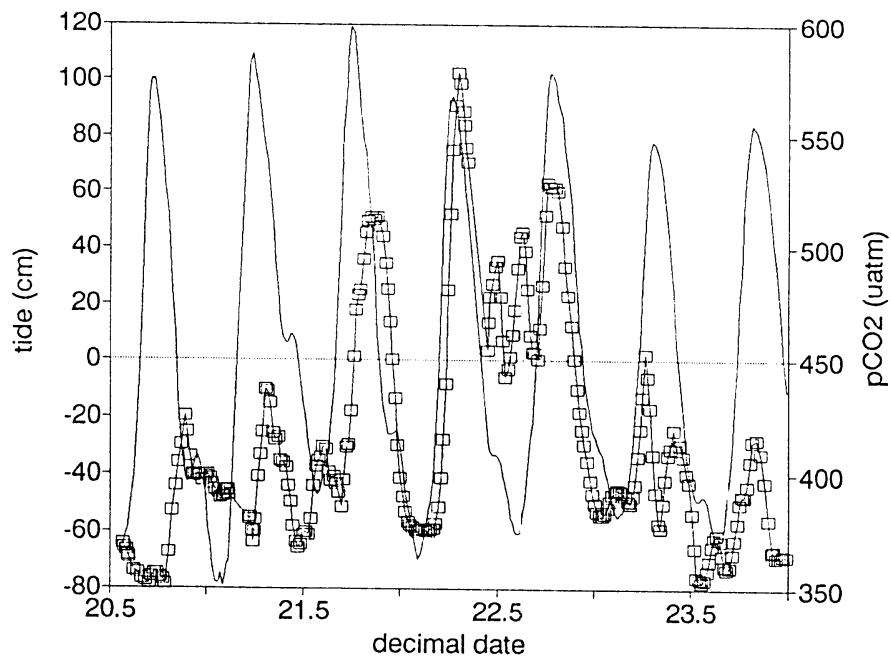


Fig.3 Time series of pCO₂ (open squares) and tidal height for the period September 20-23, 1993.

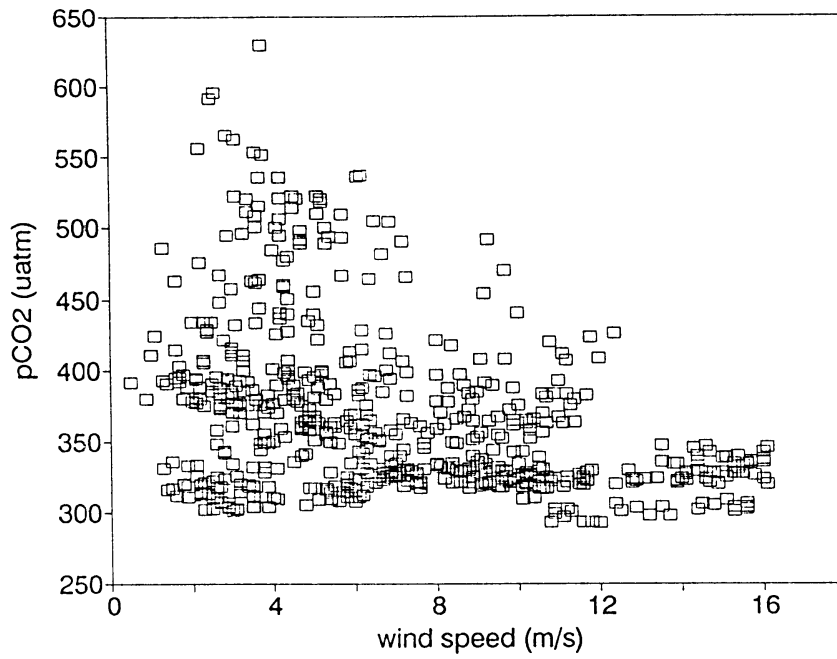


Fig.4 pCO₂ as a function of the 10m wind speed for the period September 20-29, 1993.

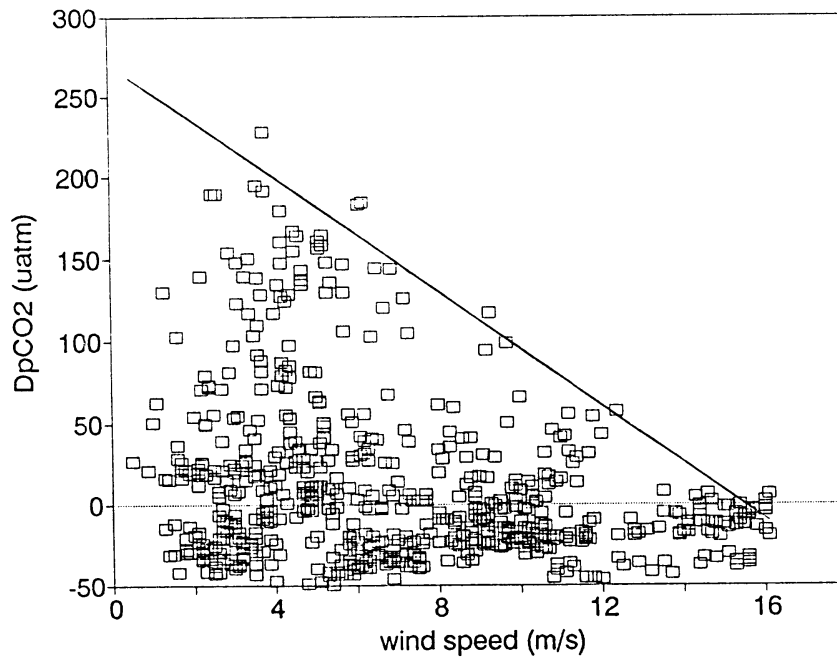


Fig.5 As fig.4, for DpCO₂. The solid line is an approximation to the upper limit of the data.

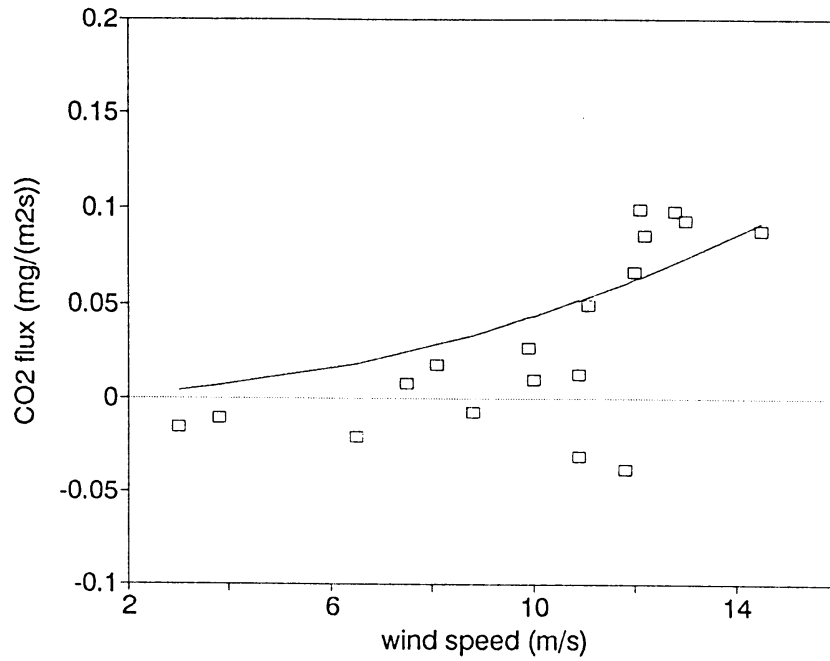


Fig.6 As fig.1; the solid line is the flux according to Wanninkhof (1992), with $DpCO_2 = 272 \mu\text{atm}$.

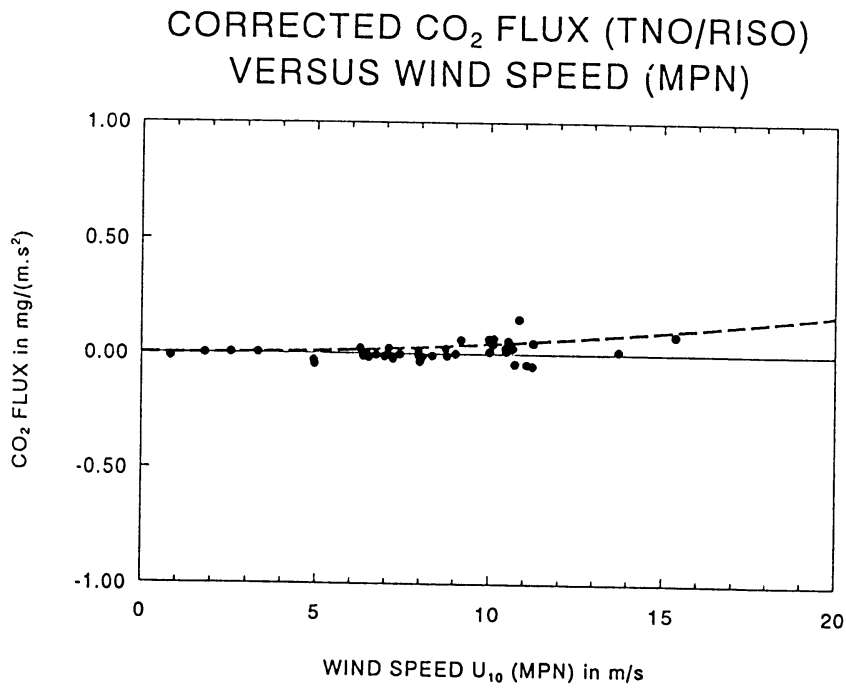


Fig.7 As fig.6, for the CO₂ flux data measured by FEL-TNO.

Investigating transport processes through the marine microlayer by passive thermal and radiometric methods

by

David K Woolf

Department of Oceanography
University of Southampton
Highfield, Southampton
United Kingdom

It is widely agreed that in rough water conditions the transfer velocity of direct exchange of a gas will be proportional to the square root of its diffusion constant or,

$$K_o \propto Sc^{-0.5} \quad \text{where,}$$

$$Sc = v/D_g$$

(Sc is the Schmidt number, D_g is the molecular diffusion constant of the gas).

In conditions of forced convection, the "Saunders" parameterisation (Saunders, 1967) is used to express bulk-skin temperature differences, ΔT, as a function of heat flux, Q:

$$\Delta T = \lambda Q v / (c_p \rho D_h u^*)$$

However, one can rewrite this equation in terms of a transfer velocity for heat,

$$K_h = u^* D_h / (\lambda v)$$

It is expected that,

$$K_h \propto Pr^{-0.5} = (v/D_h)^{-0.5}$$

Recently, Soloviev and Schluessel (1994) have applied a surface renewal model to heat and gas transfer across the sea surface. Here, we apply the simplest "horizontally homogenous" boundary-layer model for a free surface. In this case,

$$K_h Pr^{0.5} = K_o Sc^{0.5}$$

and we can deduce values of gas transfer velocity (we chose the usual standard of a Schmidt number of 600) from values of the Saunders parameter, λ , at various wind speeds:

$$K_{600} = u_* / [\lambda(600Pr)^{0.5}]$$

We have calculated transfer velocities from the $\lambda(U)$ values reported by Grassl (1976), Schluessel *et al.* (1990) and by Donlon and Woolf (1994) and these are plotted along with two of the most referenced parameterisations for the total transfer velocity, K_T (Liss and Merlivat, 1986; Tans *et al.*, 1990) in the Figure.

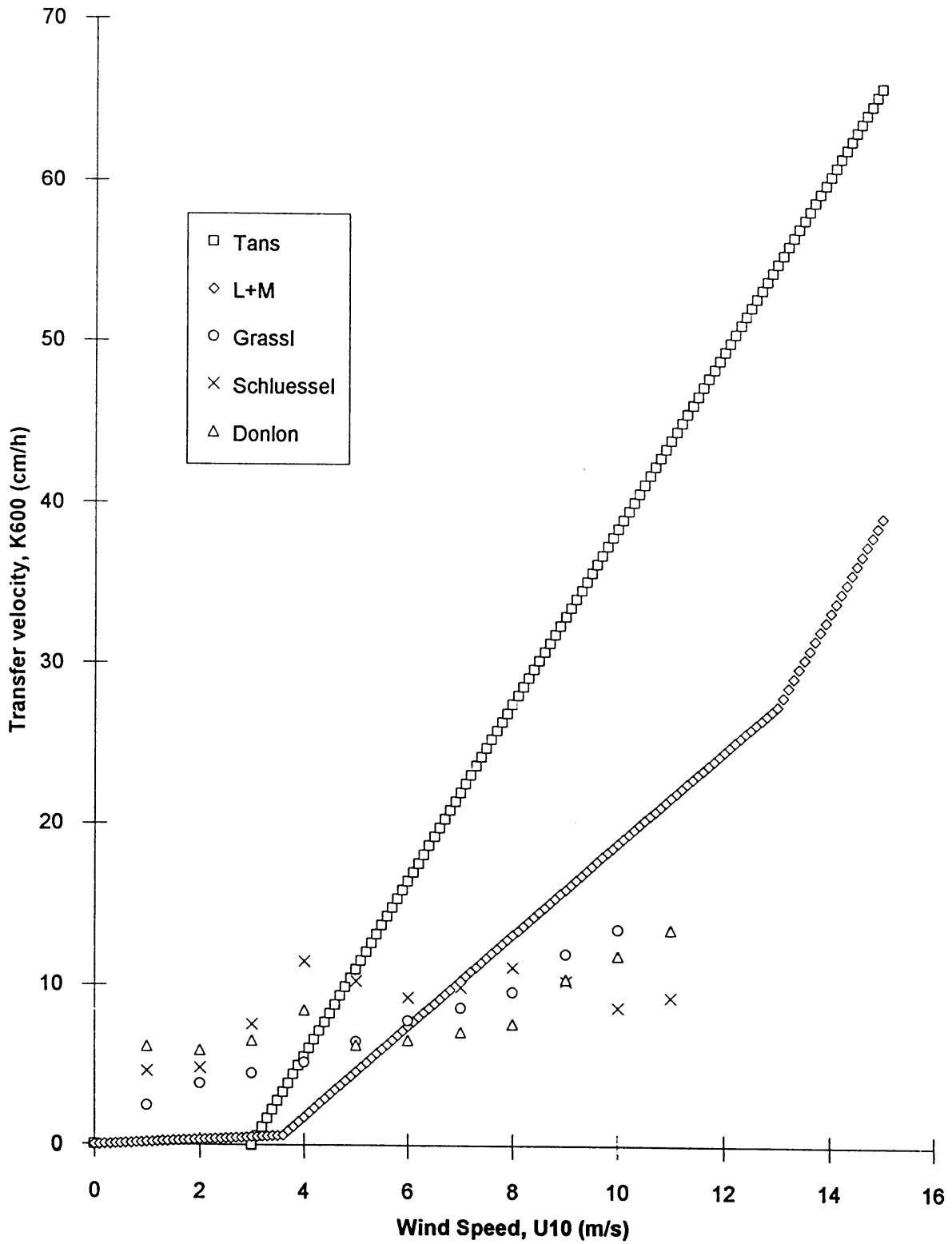
The difference between these two sets is enormous. The difference at high wind speeds may be entirely or partly due to the additional contribution of bubble-mediated transfer, K_b . Nevertheless, the weak or non-existent increase in transfer velocity with wind speed at high wind speeds inferred from the thermal skin effect is surprising, though it has some theoretical basis (Csanady, 1990; Soloviev and Schluessel, 1994). The forced convection parameterisation is inappropriate at low wind speeds, nevertheless convection at low wind speeds must often enhance the transfer of gases as well as heat, and this is a clear omission in current gas-exchange parameterisations.

The simple model described here is flawed, and certainly radiometric measurement of the sea surface remains technically challenging. Nevertheless, it is possible to measure heat transfer and temperature fields on small time and space scales, which are not feasible for gases. The inhomogeneity of the sea surface needs to be addressed theoretically and experimentally. Thermal imagers are capable of revealing surface patterns of flows, and breaking waves. Breaking waves are a "patchy" source of turbulence and surface disruption, while the associated foam patches alter emissivity as may surface slicks and wave-current and wave-wave interactions. The many uncertainties introduced by an unknown and variable emissivity can best be tackled by measuring the actual surface temperature with arrays of small, fast thermometric devices. The thermal signature of the sea surface is undoubtedly highly complex but radiometric and thermometric technology is sufficient to help unravel sea surface transfer processes with benefit to the understanding of air-sea gas exchange. It is proposed to carry out experiments of this kind during ASGAMAGE.

REFERENCES

- Csanady, G.T. 1990. The role of breaking wavelets in air-sea gas transfer, *J. Geophys. Res.*, *95*, 749-759.
- Donlon, C.J. and D.K. Woolf. 1994. Measurements of the thermal skin effect and applications to air-sea gas transfer. Poster paper, 2nd Intl. Conf. on air-sea interaction and on meteorology and oceanography of the coastal zone, Lisbon, Portugal, Sept 22-27 1994.
- Grassl, H. 1976. The dependence of the measured cool skin of the ocean on wind stress and total heat flux. *Boundary-Layer Meteorol.*, *10*, 465-474.
- Liss, P.S. and L. Merlivat. 1986. Air-sea gas exchange rates: Introduction and synthesis, in *The Role of Air-Sea Exchange in Geochemical Cycling*, P. Buat-Menard, Ed., Kluwer Academic Publishers, Dordrecht, Holland, 113-127.
- Saunders, P.M. 1967. The temperature at the ocean-air interface. *J. Atmos. Sci.*, *24*, 269-273.
- Schluessel, P., W.J. Emery, H. Grassl and T. Mammen. 1990. On the bulk-skin temperature difference and its impact on satellite remote sensing of sea surface temperature. *J. Geophys. Res.*, *95*, 13341-13356.
- Soloviev, A.V. and P. Schluessel. 1994. Parameterization of the cool skin of the ocean and of the air-ocean gas transfer on the basis of modelling surface renewal, *J. Phys. Oceanogr.*, *24*, 1339-1346.
- Tans, P.P., I.Y. Fung and T. Takahashi. 1990. Observational constraints on the global atmospheric CO₂ budget, *Science*, *247*, 1431-1438.

Traditional and skin-effect derived Transfer Velocities



Measurements of air-sea gas exchange using the dual tracer technique

P.D. Nightingale and R.C. Upstill-Goddard (UEA/Newcastle)

The flux of carbon dioxide (CO₂), and other gases of environmental significance across the air-sea interface, is most commonly derived from the product of the concentration difference between the surface ocean and atmosphere that drives the flux (ΔC) and a kinetic factor known as the gas transfer velocity (k) (Liss 1983). Although ΔC is a routine measurement for most gases of biogeochemical interest, k can only be estimated indirectly and it is likely to be influenced by a range of geophysical forcings including windspeed, temperature, surface films, whitecaps and bubble spectra (e.g. Broecker and Siems 1984; Goldman et al. 1988; Memery and Merlivat 1985; Monahan and Spillane 1984).

Three parameterisations are commonly used to estimate k from the observed windspeed (Figure 1). The Liss and Merlivat relationship (LM) was based on results obtained from a lake experiment using the purposefully added tracer sulphur hexafluoride (SF₆) and a laboratory study for high windspeeds. The parameterisation proposed by Wannikhof (1992) was essentially a quadratic curve fitted such that when averaged over the range of global windspeeds it was in agreement with the value derived from the global mean uptake of bomb-derived radiocarbon (¹⁴C) by the oceans. Similarly, Tans et al. (1990) adjusted the linear relationship of Smethie et al. (1985) to fit through the ¹⁴C point. Clearly there are drawbacks to both types of approach. Oceanic gas exchange rates may well be different to those observed in tanks and lakes where waves are small and bubbles and spray are generally absent. Equally, although the ¹⁴C method should allow a reasonable estimate of the globally averaged CO₂ uptake by the oceans, it yields little information on how k might vary in time and space, or indeed how to calculate k for other gases.

We have previously described how a dual tracer technique utilising SF₆ and ³He as a volatile tracer pair can be used to obtain estimates of k at sea (Upstill-Goddard et al. 1991, Watson et al. 1991). These early results are also shown in Figure 1. Further measurements of k using this technique in two field investigations during February 1992 and February 1993 have been made as part of the CEC-funded EPOCH and ESCOBA projects. The tracer release site, close to MPN, was specifically chosen because, at this time of year, the water column was fully mixed to the seafloor eliminating the need to budget for tracer loss across the thermocline. On each occasion approximately 100 km² of seawater was enriched with a total of 0.3 moles SF₆ and 0.05 moles ³He and the change in the ratio of ³He/SF₆ in the patch was monitored for periods of up to 10 days. Estimates of k were derived from the change in this ratio and results from all four UK dual tracer experiments are plotted against the windspeed data from MPN provided by KNMI (Figure 2). Unfortunately there are two main difficulties in using the dual tracer technique to estimate k for CO₂. One inherent drawback is that k is determined for an inert tracer and not for the gas of interest i.e. CO₂. Secondly, if ³He and SF₆ are employed as the tracer pair then the technique actually measures the difference in the transfer velocities of the two gases i.e. $k_{3\text{He}} - k_{\text{SF}_6}$. Traditionally k has been related to a power law dependence on the Schmidt number (Sc) shown below

$$k_{\text{SF}_6}/k_{3\text{He}} = (Sc_{\text{SF}_6}/Sc_{3\text{He}})^n$$

Modelling work (Ledwell, 1984), laboratory studies (Jahne et al., 1987) and lake experiments (Watson et al., 1991) show that the value of n is expected to be -0.5 at moderate windspeeds. However, if bubbles/breaking waves are an important mechanism for gas exchange then there is likely to be an additional dependence of k on solubility (e.g. Woolf 1994). Ideally, one of the tracers used in the dual tracer technique should be non-volatile so that dilution and dispersion corrections can be made to the volatile compound thus allowing direct estimates of k to be calculated. In the

Feb. 1993 tracer release, spores of the bacterium *Bacillus globigii* var. *niger* were co-deployed with ^3He and SF_6 allowing estimates of k to be derived from three tracer pairs ($\text{SF}_6/{}^3\text{He}$, ${}^3\text{He}/\text{spores}$, $\text{SF}_6/\text{spores}$). These are in good agreement and suggest that a Sc dependence of -0.5 is appropriate for SF_6 and ${}^3\text{He}$.

The average mean value for k_{CO_2} calculated from the $\text{SF}_6/{}^3\text{He}$ data, ignoring any departure from $n = -0.5$ due to bubble effects, and using a normalised Rayleigh distribution for global winds together with the Hoover and Berkshire (1969) model for the chemical enhancement of CO_2 transfer is 15.2 cm hr^{-1} for the North Sea data and 16.5 cm hr^{-1} when the recent data from a dual tracer release on the Georges Bank (Wanninkhof et al. 1993) is included in the total dataset. The LM parameterisation gives a value of 13.4 cm hr^{-1} compared to the ${}^{14}\text{C}$ derived value of 23 cm hr^{-1} . Recently, it has been suggested that the oceanic ${}^{14}\text{C}$ inventory is inconsistent with atmospheric ${}^{14}\text{C}$ records (Hesshaimer et al. 1994). These workers suggested that the k_{CO_2} derived from ${}^{14}\text{C}$ should be lowered by 25% (i.e. to 17.3 cm hr^{-1}) considerably closer to our 'best' estimate of 16.5 cm hr^{-1} .

Future dual and triple tracer releases timed to coincide with the experimental work on MPN as part of ASGAMAGE would be of great value. Firstly, urgently required information on the relative roles of windspeed, waves and bubbles and bubble spectra in air-sea gas exchange will be obtained, allowing k_{CO_2} to be more accurately predicted from the dual tracer results. Secondly, a comparison between the inert tracers and the micrometeorological techniques to be used on MPN will be of great value as the latter involve the direct determination of CO_2 fluxes over very short time-scales and have the potential to be the preferred approach for determining fluxes across the air-sea interface in the future.

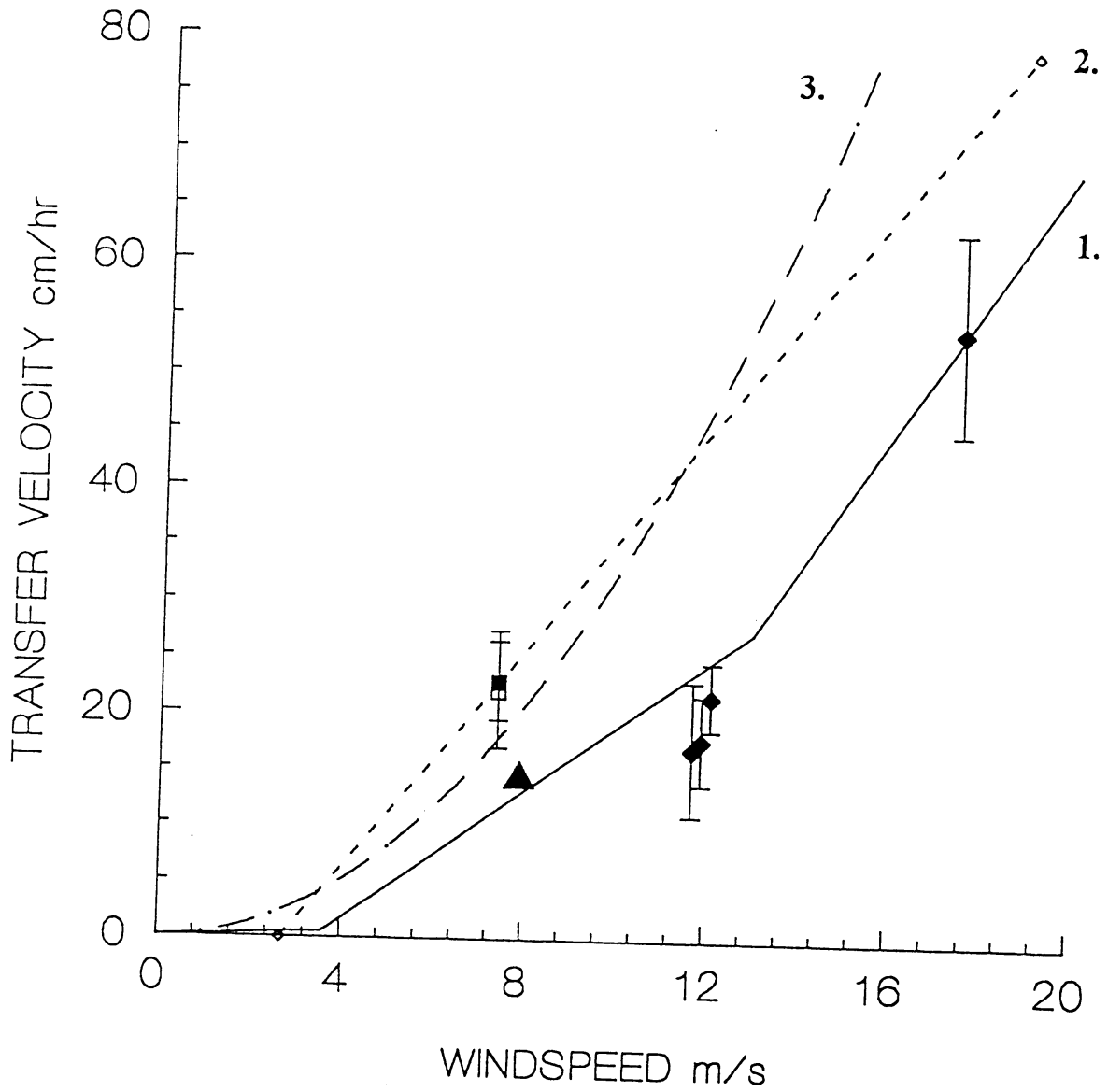
References

- Broecker H.C. and W. Siems, (1984), The role of bubbles for gas transfer from water to air at higher windspeeds: Experiments in the wind/wave facility at Hamburg, in, Gas transfer at water surfaces, eds. W. Brutsaert and G.H. Jirka, Reidel.
- Goldman J.C., M.R. Dennett and N.M. Frew, (1988), Surfactant effects on air-sea gas exchange under turbulent conditions, *Deep Sea Res.* 35 1953-1970.
- Hesshaimer V, M. Heimann and I. Levin, (1994) Radiocarbon evidence for a smaller oceanic carbon dioxide sink than previously believed, *Nature* 370 201-203.
- Hoover T.E. and D.C. Berkshire (1969) Effects of hydration in carbon dioxide exchange across an air-water interface, *J. Geophys. Res.* 74 456-464 1969.
- Jahne B., K.O. Munnich, R. Bosinger, A. Dutzi, W. Huber and P. Libner (1987), On the parameters influencing air-water gas exchange, *J. Geophys. Res.* 92 1937-1949.
- Ledwell J.J., (1984) The variation of the gas transfer velocity with molecular diffusivity, in; Gas transfer at water surfaces, eds. W. Brutsaert and G.H. Jirka, Riedel.
- Liss P.S. and L. Merlivat, (1986), Air-sea gas exchange rates: Introduction and synthesis, in; The role of air-sea exchange in geochemical cycling, ed. P. Buat-Menard, Reidel.

- Memery L. and L. Merlivat, (1985), Modelling of gas flux through bubbles at the air-water interface, *Tellus*, 37B 272-285.
- Monahan E.C. and M.C. Spillane, (1984), The role of oceanic whitecaps, in; *Gas transfer at water surfaces*, eds. W. Brutsaert and G.H. Jirka, Riedel
- Smethie W.M., T. Takahashi, D.W. Chipman and J.R. Ledwell, (1985), Gas exchange and CO₂ flux in the tropical Atlantic ocean determined from ²²²Rn and CO₂ measurements, *J. Geophys. Res.* 90 7005-7022.
- Tans P.P, I.Y. Fung and T. Takahashi, (1990), Observational constraints on the global atmospheric CO₂ budget. *Science* 247 1431-1438.
- Upstill-Goddard R.C., A.J. Watson, J. Wood and M.I. Liddicoat, (1991), Sulphur hexafluoride and helium-3 as seawater tracers: deployment techniques and continuous analysis of SF₆. *Analytica Chimica Acta* 249 555-562.
- Wanninkhof R., (1992), Relationship between wind speed and gas exchange over the ocean, *J. Geophys. Res.* 97 7373-7382.
- Wanninkhof R., W. Asher, R. Weppernig, H. Chen, P. Schlosser, C. Langdon and R. Sambrotto, (1993), Gas transfer experiment on Georges Bank using two volatile deliberate tracers *J. Geophys. Res.* 98 20237-20248.
- Watson A.J., R.C. Upstill-Goddard and P.S. Liss, (1991), Air-sea gas exchange in rough and stormy seas measured by a dual tracer technique, *Nature* 349 145-147

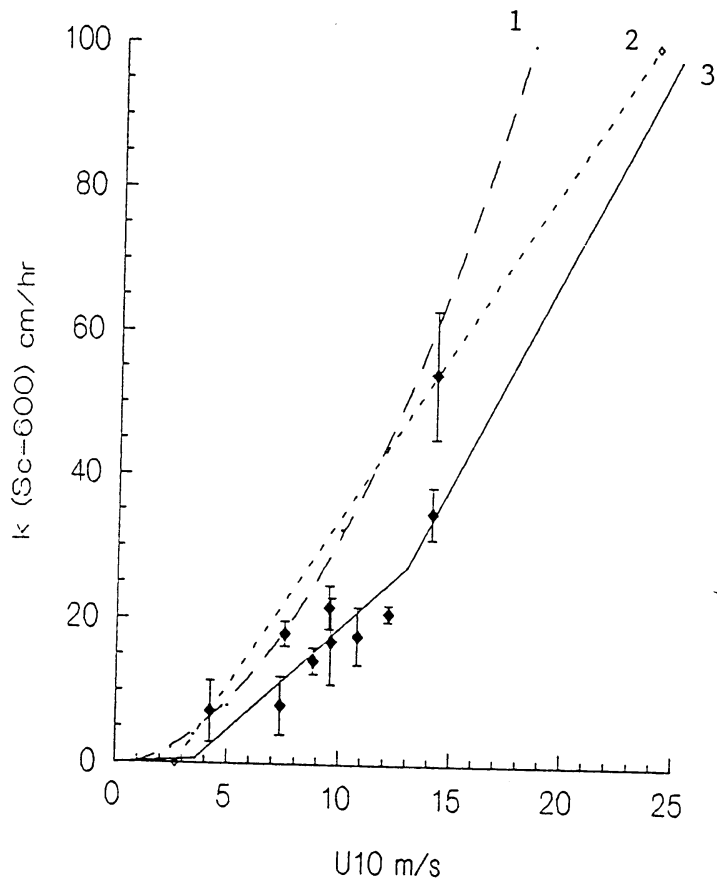
FIGURE 1

SUMMARY OF PROPOSED PARAMETERISATIONS OF THE
TRANSFER VELOCITY



Wanninkhof 1992	3.	■	14C
Smethie et al. 1985	2.		
Liss and Merlivat 1986	1.	▲	Radon
		◆	SF ₆ / ³ He

FIGURE 2
SUMMARY OF GAS TRANSFER RESULTS



- 1 = Wannikhof (1992)
- 2 = Tans et al. (1990)
- 3 = Liss and Merlivat (1986)

Workshop ASGASEX/ASGAMAGE

Annex 1

October 3-5, 1994
KNMI, de Bilt, the Netherlands

Monday, October 3

9.00 - 9.25 Welcome and coffee.

9.25 - 9.30 Opening of the workshop.

Session 1: Eddy flux measurements during ASGASEX.

9.30 - 10.00 *Bob Anderson (BIO):*
A system for measurement and analysis of eddy fluxes of CO₂, H₂O, heat and momentum at the sea surface.

10.00 - 10.30 *Wim Kohsiek (KNMI):*
Measurement and analysis of CO₂ eddy fluxes with the KNMI sensor system.

10.30 - 11.00 *Gerrit de Leeuw (TNO-FEL):*
CO₂ flux measurements during ASGASEX (with S.E.Larsen).

11.00 - 11.30 *Stu Smith & Bob Anderson (BIO):*
BIO Analysis of CO₂ and H₂O flux in ASGASEX '93.

11.30 - 12.00 Discussion of eddy flux results.

12.00 - 13.00 lunch

Session 2: Other ASGASEX results.

13.00 - 13.30 *Dorothee Bakker (NIOZ):*
CO₂ air-sea exchange as determined by indirect flux measurements.

13.30 - 14.00 *Hein de Wilde (NIOZ):*
Air-sea exchange of nitrous oxide and methane at Meetpost Noordwijk.

14.00 - 14.30 *Gerrit de Leeuw (TNO-FEL):*
Bubble and aerosol measurements (with L.H.Cohen).

14.30 - 15.00 coffee, tea.

15.00 - 15.30 *Marcel Cure and Peter Bowyer (UCG):*
Sonar study of surface turbulence.

15.30 - 16.00 *David Woolf (USDO):*
Bubbles and vertical transport below the sea surface.

16.00 - 16.30 *Wiebe Oost (KNMI):*
Trying to (make it) make sense.

16.30 - 17.00 General discussion ASGASEX '93 results

17.00 End of day 1.

Tuesday, October 4

9.00 - 10.00 General discussion ASGASEX '93 results (cont.)

10.00 - 10.30 Publication policy, identification papers and authors.

Session 3. What do we need in ASGAMAGE?

10.30 - 11.00 *Wiebe Oost (KNMI):*

The consequences of ASGASEX '93 results for ASGAMAGE (with interruptions from other workshop participants).

11.00 - 11.30 *David Woolf (USDO):*

Investigating transport processes through the marine microlayer by passive thermal and radiometric methods.

11.30 - 12.00 *Phil Nightingale (UEA):*

Measurements of air-sea gas exchange using the dual tracer technique.

12.00 - 13.00 lunch

13.00 - 14.30 **Who/what else ?**

Information about other potential participants, their methods, equipment, goals and requirements.

14.30 - 15.00 coffee, tea

Session 4: Logistic planning of ASGAMAGE.

15.00 - 17.00

What parameters do you/we need ?

Which of them are needed simultaneously ?

What requirements do you/we have regarding time of the year, platform, space, mains, sea water, plumbing, lab temperature ?

What are the consequences in terms of platform and ship availability ?

What else ?

How, for heavens sake, do we accomodate all this in a decent way ?

What additional meetings do we need ?

17.00

End of day 2.

Wednesday, October 5

Session 4: Logistic planning of ASGAMAGE (cont.)

9.00 - 10.00 Scheduling.
Draft experimental plan with time scheme.

Session 5: Financial planning

10.00 - 10.30 *Wiebe Oost (KNMI):*
Expenses involved in the experiment proper.

10.30 - 11.30 Identification of funding problems.
Identification of funding agencies.
Identification of possible common proposals.
Arrangements for submission of proposals.

11.30 - 12.00 Summary of arrangements.

12.00 End of workshop.

Annex 2. Institute acronyms and participants.

AEK Risø: Risø National Laboratory (*not represented*)
Dr.S.Larsen, Mr.F.Hansen
Postboks 49, DK-4000 Roskilde, Denmark

BIO: Bedford Institute of Oceanography, Ocean Circulation Division
Dr.S.D.Smith, Mr.R.J.Anderson
P.O. Box 1006, Dartmouth, N.S., Canada B2Y 4A2

IOS-Can.: Institute of Ocean Sciences (*not represented*)
Dr.D.Farmer
P.O.Box 6000, Sidney, British Columbia V8L 4B2, Canada

IOS-UK: Institute of Oceanographic Sciences, Deacon Laboratory (*not represented*)
Mr.A.Hall
Brook Road, Wormley, Godalming Surrey GU8 5UB, UK

KNMI: Royal Netherlands Meteorological Institute
Dr.W.A.Oost, Dr.W.Kohsiek, Mr.E.H.W.Worrell, Mr.C.van Oort
P.O.Box 201, 3730 AE De Bilt, the Netherlands

MPIC: Max Planck Institut für Chemie, Abteilung Biochemie
Dr.S.Rapsomanikis
Postfach 3060, D-6500 Mainz, Germany

NIOZ: Netherlands Institute for Sea Research
Prof.H.J.W.de Baar, Mw.Ir.D.C.E.Bakker, Ir.H.de Wilde, Dr.M.Stoll
P.O.Box 59, 1790 AB Den Burg, the Netherlands

NOAA Boulder: NOAA Environmental Research Laboratory
Dr.Ch.W.Fairall
325 Broadway, Boulder CO 80303, USA

NOAA Miami: NOAA-AOML, Ocean Chemistry Department
Dr.R.Wanninkhof
4301 Rickenbacker Causeway, Miami FL 33149, USA

SUDO: Southampton University, Department of Oceanography
Dr.D.K. Woolf
the University, Highfield, SOUTHAMPTON S09 5NH, United Kingdom

TNO-FEL: TNO-Physics and Electronics Laboratory
Dr.G.J.de Leeuw, Ir.G.Kunz
P.O. Box 96864, 2509 JG Den Haag, the Netherlands

UCG: University College Galway, Department of Oceanography
Dr.M.Cure
Galway, Ireland

UEA: University of East Anglia, School of Environmental Sciences
Dr.P.Nightingale
Norwich NR4 7TJ, United Kingdom